

1 **The varying Earth's radiative feedback connected to the ocean energy**
2 **uptake: a theoretical perspective from conceptual frameworks**

3 Diego Jiménez-de-la-Cuesta

4 *Max-Planck-Institut für Meteorologie, Hamburg, Deutschland*

5 *Corresponding author:* Diego Jiménez-de-la-Cuesta, diego.jimenez@mpimet.mpg.de This work
6 has been submitted to the *Journal of Climate*. Copyright in this work may be transferred without
7 further notice.

8 ABSTRACT: When quadrupling the atmospheric CO₂ concentration in relation to pre-industrial
9 levels, most global climate models show an initially strong net radiative feedback that significantly
10 reduces the energy imbalance during the first two decades after the quadrupling. Afterwards,
11 the net radiative feedback weakens, needing more surface warming than before to reduce the
12 remaining energy imbalance. Such weakening radiative feedback has its origin in the tropical
13 oceanic stratiform cloud cover, linked to an evolving spatial pattern of surface warming. In
14 the classical linearized energy balance framework, such variation is represented by an additional
15 term in the planetary budget equation. This additional term is usually interpreted as an ad-hoc
16 emulation of the cloud feedback change, leaving unexplained the relationship between this term
17 and the spatial pattern of warming. I use a simple non-linearized energy balance framework to
18 justify that there is a physical interpretation of this term: the evolution of the spatial pattern of
19 warming is explained by changes in the ocean's circulation and energy uptake. Therefore, the
20 global effective thermal capacity of the system also changes, leading to the additional term. In
21 reality, the clouds respond to what occurs in the ocean, changing their radiative effect. In the
22 equation, the term is now a concrete representation of the ocean's role. Additionally, I derive for
23 the first time an explicit mathematical expression of the net radiative feedback and its temporal
24 evolution in the linearised energy balance framework. This mathematical expression supports the
25 new proposed interpretation. As a corollary, the twenty-year time scale used to study the variation
26 of the net radiative feedback becomes justified.

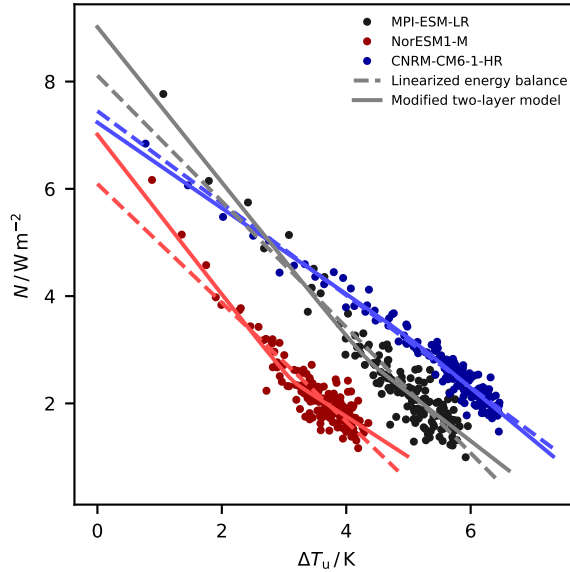
27 SIGNIFICANCE STATEMENT: Linearized energy balance models have helped the study of
28 Earth's radiative response. However, the present linear models are at the edge of usefulness to get
29 more insights. In this work, I justify that part of the non-linearity can be explained without peculiar
30 atmospheric radiative feedback mechanisms or a non-linearity in the radiative response. Instead,
31 the concept of an evolving thermal capacity recovers the ocean's role in redistributing the energy,
32 changing the spatial warming pattern, and, finally, altering the atmospheric feedback mechanisms.
33 This work also justifies the timescales used in the field for studying the variation of net radiative
34 feedback.

35 1. Introduction

36 The principle of conservation of energy has provided an important tool to study Earth's climate
37 (e.g., Fourier 1827; Arrhenius 1896; Callendar 1938; Budyko 1969; Hansen et al. 1985; Senior
38 and Mitchell 2000; Gregory et al. 2004; Hansen et al. 2010). At the top of the atmosphere (TOA),
39 the incoming radiative flux should balance the outgoing radiative flux, leading to a zero net change
40 of the Earth's energy content (E). If we perturb the radiative balance, the Earth system will change
41 its energy content: this is the radiative forcing (F). Consequently, the surface temperature (T_u)
42 will also change, reducing the imbalance. Other variables that define the state of the Earth system
43 also adjust after a surface temperature change, leading to variations in the planetary albedo or the
44 outgoing long-wave radiation, and further altering the TOA net radiative flux. These mechanisms
45 are the radiative feedback mechanisms that generate the radiative response (R) to the forcing. The
46 balance just described can be summarized in an equation

$$N = F + R \quad (1)$$

47 where $N = \dot{E}$ is the time derivative of the energy content. N is also called the TOA radiative
48 imbalance. A radiative feedback mechanism is negative if it reduces the radiative imbalance.
49 Present Earth's climate has a negative net radiative feedback. Therefore, the radiative response
50 stabilizes the system under forcing at the expense of surface temperature changes: the climate
51 sensitivity. Thus, the more negative the net radiative feedback is, the smaller the surface temperature
52 change is. We can visualize how negative is the net radiative feedback with a NT -diagram: a



55 FIG. 1. NT -diagram for three GCMs forced with a quadrupling of the atmospheric CO_2 concentration.
 56 Dots, annually- and globally-averaged TOA radiative imbalance plotted versus the surface temperature change in
 57 relation to the pre-industrial control state. Dashed lines, a linear regression estimate for the relationship between
 58 N and ΔT_u . Continuous lines, fit using the modified two-layer model. The model in red presents a large variation
 59 in the net radiative feedback, as shown by the strong curvature of the relationship between N and ΔT_u . The net
 60 radiative feedback weakens as the system evolves. The model in grey shows a slight curvature. The model shown
 61 in blue has a reversed curvature, which means that the net radiative feedback strengthens as the system evolves.

53 plot of N versus ΔT_u (Figure 1). The slope of the diagram is the magnitude of the net radiative
 54 feedback. The problem is giving R a functional form in terms of variables that describe the system.

62 Several studies have used equation (1) together with NT -diagrams for successfully studying
 63 the radiative response and the equilibrium climate sensitivity to CO_2 forcing (ECS) as shown in
 64 global climate models (GCMs) and the historical record. Given the quasi-linearity found in the
 65 NT -diagrams of GCMs forced with a quadrupling of the pre-industrial atmospheric CO_2 and
 66 assuming that R is only a function of T_u , most of these studies implicitly used a Taylor series of R
 67 truncated at its first-order term (popularized by Gregory et al. 2004). Consequently, they assumed
 68 that (1) the climate state used as the basis for the Taylor series is in balance, and (2) the changes in
 69 T_u due to the CO_2 forcing are small enough to neglect higher-order terms of the series. The result

70 is

$$N \approx F + \left. \frac{dR}{dT_u} \right|_{T_u=T_u^*} \Delta T_u \quad (2)$$

71 where T_u^* is the surface temperature in the reference climate state, and ΔT_u are the anomalies around
 72 this reference state. The evaluated derivative is usually called the climate feedback parameter λ ,
 73 representing an approximation to the magnitude of the net radiative feedback and leading to the
 74 more clean equation

$$N \approx F + \lambda \Delta T_u \quad (3)$$

75 Under these strong assumptions, one obtains λ and F estimates from the NT -diagrams or observa-
 76 tions. Afterwards, using equation (3) one then estimates ECS. This estimate is important in GCMs,
 77 as models usually are not run to the equilibrium. However, the linearity assumptions break: in
 78 most GCMs, the net radiative feedback becomes less negative as the system warms in timescales of
 79 around twenty years. Thus, the ECS is underestimated when using such linearization (Rugenstein
 80 and Armour 2021). More importantly, this variation indicates two options: (a) the non-linearity in
 81 $R(T_u)$ is important and (b) state variables other than T_u are also important for calculating R .

82 Some authors extended the framework of equation (3) to accommodate this effect (Held et al.
 83 2010; Winton et al. 2010; Geoffroy et al. 2013b,a). First they introduced two layers: a) the upper
 84 layer that includes the atmosphere and the ocean's mixed layer, and b) the deep ocean's layer.
 85 Therefore, the state variables are now the surface (T_u) and the deep-ocean (T_d) temperatures. These
 86 two layers greatly differ on thermal capacities, introducing two timescales: the fast upper layer and
 87 the slow deep layer. They connected both layers with the deep ocean's energy uptake (H), which
 88 should depend on $T_u - T_d$. However, they also introduced a perturbed energy uptake in the upper
 89 layer H' to account for the change in the radiative response

$$\begin{cases} N_u \approx F + \lambda \Delta T_u - H' \\ N_d \approx H \end{cases} \quad (4)$$

$$N = N_u + N_d \approx F + \lambda \Delta T_u + (H - H') \quad (5)$$

90 where the term $H - H'$ translates the concept of the varying feedback to a problem of variation of
91 the deep ocean's energy uptake. Equations (4) and the corresponding planetary budget correctly
92 represent a varying climate feedback parameter. However, some interpreted $H - H'$ as an additional
93 radiative feedback mechanism from equation (5). Nonetheless, this perspective presents the new
94 term $H - H'$ as devoid of any physical meaning, apparently rendering the conceptual framework
95 as flawed.

96 Observations suggest that the net radiative feedback changes in response to an evolving spatial
97 pattern of surface warming (Zhou et al. 2016; Mauritsen 2016; Ceppi and Gregory 2017). The
98 pattern alters the atmospheric stability in decadal timescales, modifying the tropical stratiform
99 clouds' contribution to the short-wave radiative response. In the early decades after the forcing in
100 GCMs, the surface mildly warms in subsidence regions, whereas the deep convection warms the
101 free troposphere. More warming aloft than below enhances the boundary-layer inversion, leading
102 to more stratiform cloud cover and reflected short-wave radiation. After the first decades, there is
103 more warming below than aloft, leading to a weaker inversion, less stratiform cloud cover, and less
104 reflected short-wave radiation. This mechanism suggests that the varying net radiative feedback
105 originates from a process that depends on more than surface warming. Furthermore, several
106 modeling studies found that warming in specific regions leads to a more negative net feedback than
107 when applying warming in other regions.

108 Inspired by earlier views on the term $H - H'$ as a perturbed thermal capacity and in new studies
109 that connect ocean energy uptake and the regional warming patterns, I show why this term cannot
110 be seen as a peculiar atmospheric radiative feedback mechanism but as a changing thermal capacity.
111 The evolving warming pattern is consistent with a changing oceanic circulation that redistributes
112 the energy, gradually changing the surface temperature and, as a result, the radiative feedback
113 mechanisms. The global effect is as if the thermal capacity of the system changes. First, I show the
114 consistency of the idea by using a non-linear version of equation (1). Second, I derive for the first
115 time a mathematical expression for the magnitude of the net radiative feedback in NT -diagrams,
116 using the explicit solutions of the linear ordinary differential equations (4) in terms of their normal
117 modes. I find that the variation of the net radiative feedback depends on the ratio of the change
118 in the energy content between the upper and deep layers. This fact further shows that a changing
119 effective thermal capacity explains better the variation of the net feedback, even in the case of

120 equation (4). As a corollary, I show that the twenty-year timescale for evaluating the pattern effect
121 can be justified by the expression I have derived.

122 2. Theory

123 a. Non-linear framework

124 If E is the Earth's energy content, then its change $N = \dot{E}$ should equal the difference between
125 the TOA incoming and outgoing radiative fluxes. Let us write the incoming TOA radiative flux in
126 terms of the solar incoming radiative flux $S := S(t)$, the planetary albedo α , and the net radiative
127 flux coming from other natural or anthropogenic sources $G := G(t)$. We approximate the outgoing
128 radiative flux as that of a grey-body of emissivity ϵ at the emission temperature $T_e = fT_u$, where f
129 is the lapse-rate scaling factor that relates surface temperature T_u to T_e . With these elements, the
130 planetary energy budget is

$$N = (1 - \alpha)S + G - \epsilon\sigma(fT_u)^4 \quad (6)$$

131 where α , ϵ , and f are functions of variables that describe the system. The planetary albedo depends
132 on the cloud types and cover and the cryosphere extent. Thus, the planetary albedo can depend
133 on the surface temperature and the cloud liquid water content (q_{cw}) or, $\alpha := \alpha(T_u, q_{cw}, \dots)$. In
134 the case of the emissivity and the lapse-rate scaling factor, the relevant quantity should be the
135 amount of water vapor (q_v), additionally to T_u and q_{cw} . Therefore, $\epsilon := \epsilon(T_u, q_v, q_{cw}, \dots)$ and
136 $f := f(T_u, q_v, q_{cw}, \dots)$. The atmospheric radiative feedback mechanisms are contained in α , ϵ ,
137 and f . As the state variables evolve, α , ϵ , f change and, consequently, the TOA net radiative flux.

138 The interpretation of $H - H'$ in equation (5) as a atmospheric radiative feedback is completely ad-
139 hoc in the context of equation (6). If we included $H - H'$ in α , ϵ , or f , another hidden state variable
140 would enter the definition of α , ϵ , or f . Directly claiming for regional temperature features in the
141 surface temperature as the hidden variable is not an option since the model is globally averaged.
142 Therefore, one runs out of options to assign a definite physical meaning to $H - H'$ in terms of
143 radiative feedback mechanisms.

144 The original idea behind $H - H'$ is that the effect of the evolving spatial pattern of warming
145 is connected to a change in the deep ocean's energy uptake. In other words, one temporarily is

146 storing much more energy than expected in the deep ocean, allowing the surface to warm less. As
 147 time passes, this larger-than-expected energy uptake is not possible anymore due to changes in the
 148 ocean circulation, leading to a different surface warming distribution, which is characteristic of the
 149 new ocean state. Therefore, a regional differential warming produced by a new ocean circulation
 150 state has a global effect. Consequently, $H - H'$ is an expression of the change in the ocean
 151 energy distribution and can be expressed as a change in the global thermal capacity of equation
 152 (6). Therefore, this thermal capacity is the effective thermal capacity associated with the ocean
 153 circulation.

154 Precisely, the planetary thermal capacity is present in the energy content: $E = CT_u$. If C
 155 is constant, then $N = \dot{E} = C\dot{T}_u$. Defining $N := C\dot{T}_u$ and introducing the varying C results in
 156 $\dot{E} = C\dot{T}_u + \dot{C}T_u = N + \dot{C}T_u$. Thus, the planetary energy budget has the new form

$$N = (1 - \alpha)S + G - \epsilon\sigma(fT_u)^4 - \dot{C}T_u \quad (7)$$

157 In this expression, the last term is a version of the linearized $H - H'$ term in equation (5). Therefore,
 158 in this perspective, the perturbed ocean energy uptake is not an exceptional atmospheric radiative
 159 feedback, has a definite physical interpretation, and connects the spatial pattern of warming with a
 160 changing ocean circulation.

161 *b. The modified linearized two-layer model*

162 I will now use the modified linearized two-layer model to derive an explicit mathematical
 163 expression for the net radiative feedback. With this mathematical expression, I find that the traces
 164 of the relationship of the pattern effect with ocean circulation are present even in this linearized
 165 energy budget. The following equations define the modified linearized two-layer model (Geoffroy
 166 et al. 2013a)

$$\begin{cases} C_u \frac{d \Delta T_u}{dt} = F + \lambda \Delta T_u - \hat{\epsilon} \gamma (\Delta T_u - \Delta T_d) \\ C_d \frac{d \Delta T_d}{dt} = \gamma (\Delta T_u - \Delta T_d) \end{cases} \quad (8)$$

167 where the first equation corresponds to the upper-layer budget and the second equation to the deep
 168 layer. The parameters λ and γ are the climate feedback parameter and the rate of deep-ocean energy

169 uptake. These parameters are valid in the neighborhood of the reference climate state (T_u^*, T_d^*) . C_u
 170 and C_d are respectively the (fixed) thermal capacities of the upper and deep layers. ΔT_u and ΔT_d
 171 are the temperature anomalies referred to (T_u^*, T_d^*) . The planetary imbalance is the sum of both
 172 equations, resulting in $N = F + \lambda \Delta T_u + (1 - \hat{\varepsilon})\gamma(\Delta T_u - \Delta T_d)$. Therefore,

$$H - H' \approx (1 - \hat{\varepsilon})\gamma(\Delta T_u - \Delta T_d)$$

173 In view of equation (7), this $H - H'$ is an approximation of $\dot{C}T_u$ in the neighborhood of the reference
 174 climate state (T_u^*, T_d^*) . If the efficacy of the deep-ocean energy uptake $\hat{\varepsilon} > 1$, $H - H'$ would reduce
 175 the imbalance. If $\hat{\varepsilon} < 1$, $H - H'$ would increase the imbalance. Finally, if $\hat{\varepsilon} = 1$, there would be
 176 no pattern effect and the equations reduce to those presented by Geoffroy et al. (2013b).

177 It is better to write equations (8) in the following fashion

$$\begin{cases} \frac{d \Delta T_u}{dt} = F' + \lambda' \Delta T_u - \hat{\varepsilon} \gamma' (\Delta T_u - \Delta T_d) \\ \frac{d \Delta T_d}{dt} = \gamma'_d (\Delta T_u - \Delta T_d) \end{cases} \quad (9)$$

178 where $F' := F/C_u$ with units of K s^{-1} and, $\lambda' := \lambda/C_u$, $\gamma' := \gamma/C_u$ and $\gamma'_d := \gamma/C_d$ with
 179 units of s^{-1} . Equations (9) are a system of linear ordinary differential equations (Geoffroy et al.
 180 2013a; Rohrschneider et al. 2019). Although the solutions are standard and widely discussed in
 181 other articles (e.g. Geoffroy et al. 2013a; Rohrschneider et al. 2019), here I will use the normal
 182 mode approach. The solutions written in terms of the normal modes are more elegant and ease
 183 the algebraic transformations. In the following, I summarize the relevant facts, leaving the full
 184 mathematical discussion in the appendix A of this article.

185 The homogeneous ($F' \equiv 0$) version of the system (9) has two distinct eigenvalues $\mu_{\pm} := (\hat{\lambda} \pm \kappa)/2$,
 186 where $\hat{\lambda} := \lambda' - \hat{\varepsilon} \gamma' - \gamma'_d$ and $\kappa^2 := \hat{\lambda}^2 + 4\lambda' \gamma'_d$. These eigenvalues provide two distinct eigenvectors,
 187 forming a basis in which the full system (9) is uncoupled and, therefore, has a straight-forward
 188 solution. The eigensolutions ΔT_{\pm} are the solutions associated with each eigenvalue. Afterwards,
 189 one can return to the original representation, finding that ΔT_u and ΔT_d are linear combinations of
 190 ΔT_{\pm} . These linear combinations are the normal modes: the symmetric mode $\Delta T_s := \Delta T_+ + \Delta T_-$ and

191 the antisymmetric mode $\Delta T_a := \Delta T_+ - \Delta T_-$. The main result of this process is that $\Delta T_u = \Delta T_s$ and
 192 $\Delta T_d = \alpha \Delta T_s + \beta \Delta T_a$, where α and β are scalars that depend on the coefficients of the system (9).

193 I then write \dot{N} , the total derivative of the imbalance, in terms of the normal modes, and divide
 194 by the time derivative of ΔT_u to get an explicit mathematical expression for the magnitude of the
 195 net radiative feedback and its evolution. I reorder the terms to write the expression as a multiple
 196 of the climate feedback parameter λ . In the factor, I separate the radiative forcing (\mathcal{F}_{for}), radiative
 197 response (\mathcal{F}_{res}), and pattern effect (\mathcal{F}_{pat}) components of the magnitude

$$\begin{aligned} \lambda_t &= \frac{\dot{N}}{d \Delta T_u / dt} = (\mathcal{F}_{\text{for}} + \mathcal{F}_{\text{res}} + \mathcal{F}_{\text{pat}}) \lambda \\ &= \left[\mathcal{F}_{\text{for}} + \mathcal{F}_{\text{res}} + \frac{\hat{\varepsilon} - 1}{2\hat{\varepsilon}} (\mathcal{F}_{\text{pat, stat}} - \mathcal{F}_{\text{pat, dyn}}) \right] \lambda \end{aligned} \quad (10)$$

198 The \mathcal{F}_{pat} has two components: the statical ($\mathcal{F}_{\text{pat, stat}}$) and dynamical ($\mathcal{F}_{\text{pat, dyn}}$). Each term has the
 199 following expression

$$\mathcal{F}_{\text{for}} = -\frac{1}{|\lambda|} \frac{\dot{F}}{d \Delta T_s / dt} \quad (11)$$

$$\mathcal{F}_{\text{res}} = \frac{\hat{\varepsilon} + 1}{2\hat{\varepsilon}} \quad (12)$$

$$\mathcal{F}_{\text{pat, stat}} = C_u \frac{\gamma}{|\lambda|} \left(\frac{\hat{\varepsilon}}{C_u} + \frac{1}{C_d} \right) \quad (13)$$

$$\mathcal{F}_{\text{pat, dyn}} = C_u \frac{\kappa}{|\lambda|} \frac{d \Delta T_a / dt}{d \Delta T_s / dt} \quad (14)$$

200 These expressions (10) – (14) are general for any kind of forcing. One just needs the solutions in
 201 terms of normal modes to use them. Let us analyze each term.

- 202 • The forcing component (11) simply compares the evolution of F with the evolution of the
 203 surface temperature change, given that $\Delta T_u = \Delta T_s$. This component only contributes if the
 204 forcing is time-varying.

205 • The response component (12) is constant and will only give a correction to the original λ if
206 $\hat{\varepsilon} \neq 1$.

207 • The pattern effect component is only active if $\hat{\varepsilon} \neq 1$. In case it is active, we have the
208 contributions of the static and dynamic terms.

209 1. The static term (13) has three factors. One of them is a sum of the inverse of the
210 thermal capacities of the system. This arrangement is similar to the inverse of the total
211 capacitance of electric capacitors in series. Therefore, it can be interpreted as the effect
212 of the initial state of the ocean energy distribution as discussed for equation (7).

213 2. The dynamic term (14) has the ratio of the time derivatives of ΔT_s and ΔT_a . However,
214 $\Delta T_d = \alpha \Delta T_u + \beta \Delta T_a$ or $\Delta T_a = (1/\beta) \Delta T_d - (\alpha/\beta) \Delta T_u$. Therefore, the ratio of derivatives in
215 the dynamic term is a ratio of the derivatives of the deep- to the upper-layer temperature
216 anomalies plus a constant. Therefore, its is related to the ratio of the changes in energy
217 content of the deep to the upper layer.

218 One should recall that $\hat{\varepsilon} = 1$ means that there is no effect of the energy redistribution due to ocean
219 circulation changes on the surface temperature: no pattern effect. In that case, the only components
220 that contribute to equation (10) are \mathcal{F}_{for} and \mathcal{F}_{res} . It does not mean that $\mathcal{F}_{\text{pat, stat}}$ and $\mathcal{F}_{\text{pat, dyn}}$ are zero,
221 but that their effects on the net radiative feedback are absent. If this situation had been possible
222 in reality, ocean circulation and ocean energy distribution would have been decoupled from the
223 spatial pattern of warming.

224 3. Results

225 *a. The explicit slope of the NT–diagram when abruptly changing the atmospheric CO₂*

226 In the abrupt-4xCO₂ experiments, the variation of the net radiative feedback was detected as a
227 curvature in the NT–diagram. I obtain for the first time a concrete expression of the net radiative
228 feedback in those experiments, using equation (10) and the normal-mode solutions for constant

radiative forcing. The solutions provide the following form for the components (11) – (14)

$$\mathcal{F}_{\text{for}} = 0 \quad (15)$$

$$\mathcal{F}_{\text{res}} = \frac{\hat{\varepsilon} + 1}{2\hat{\varepsilon}} \quad (16)$$

$$\mathcal{F}_{\text{pat, stat}} = C_u \frac{\gamma}{|\lambda|} \left(\frac{\hat{\varepsilon}}{C_u} + \frac{1}{C_d} \right) \quad (17)$$

$$\mathcal{F}_{\text{pat, dyn}} = C_u \frac{\kappa}{|\lambda|} \tanh \left[\frac{\kappa}{2} (t - t_0) + \text{arctanh}(Z) \right] \quad (18)$$

$$Z = \frac{\hat{\lambda} + 2\gamma'_d}{\kappa} < 0 \quad (19)$$

One can notice that the time-dependent ratio in equation (14) takes a very elegant and simple form, even though the complexity of the mathematical expressions of the normal-mode solutions (appendix A).

The time-evolving part of equation (18) is an hyperbolic tangent. A plain hyperbolic tangent, $\tanh(t)$, is a monotonically increasing s-shaped or sigmoidal curve, and its possible values are between -1 and 1 , crossing zero at $t = 0$. The extreme values -1 and 1 are asymptotes. Leaving out the term $\text{arctanh}(Z)$, our function is similar to $\tanh[(\kappa/2)(t - t_0)]$. This function still has -1 and 1 as asymptotes but crosses zero at $t = t_0$. Depending on the value of $\kappa > 0$, the evolution between asymptotes would be faster. If κ were very large, the function would resemble a step function. The smaller the κ , the gentle the change of the function between asymptotes. Therefore $\kappa/2$ is a scaling factor. We conclude the analysis by adding $\text{arctanh}(Z)$. This term shifts the argument of the hyperbolic tangent. If we evaluate $\tanh[(\kappa/2)(t - t_0) + \text{arctanh}(Z)]$ at t_0 , we obtain $\tanh(\text{arctanh}(Z)) = Z < 0$. Therefore, the zero crossing is not anymore at t_0 but at a posterior time and the value of the function at t_0 is negative. I call time of sign reversal (t_{rev}) to the new time where the function becomes zero. This time is

$$t_{\text{rev}} = t_0 + \frac{2}{\kappa} \text{arctanh} |Z| \quad (20)$$

Therefore, $\mathcal{F}_{\text{pat, dyn}} < 0$ for $t_0 < t < t_{\text{rev}}$ and non-negative otherwise.

246 Since in $t_0 < t < t_{\text{rev}}$ $\mathcal{F}_{\text{pat, dyn}}$ is negative, the dynamic component strengthens the net radiative
 247 feedback, as \mathcal{F}_{pat} will be larger than without the dynamic component. Nonetheless, the net radiative
 248 feedback still becomes less negative as time evolves. In contrast, for $t > t_{\text{rev}}$ $\mathcal{F}_{\text{pat, dyn}} \geq 0$, the
 249 dynamic component now contributes to weaken even more the feedback. This means that the time
 250 of sign reversal is a new timescale in the system: before t_{rev} the dynamic component dampens
 251 the weakening of the net radiative feedback, but after t_{rev} the dynamic component promotes the
 252 weakening. This fact leads to the notable curvature of the NT -diagrams.

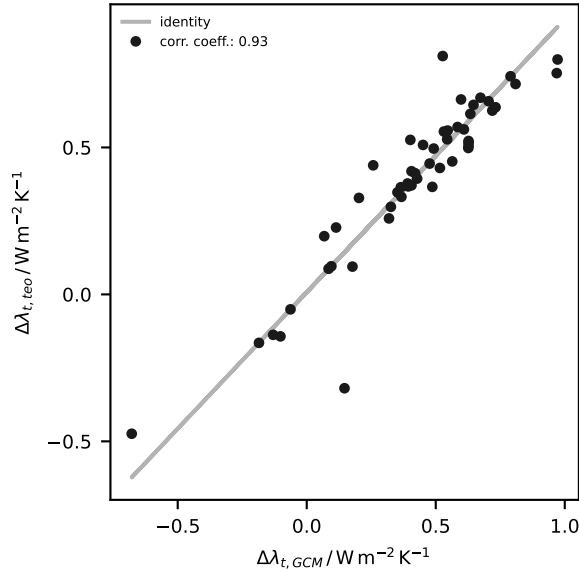
253 *b. Numerical estimates of time of sign reversal in models*

259 Following the method shown by Geoffroy et al. (2013a), I calculate the thermal, circulation and
 260 radiative parameters of the modified linearized two-layer model for a selection of 52 models of
 261 the phases 5 and 6 of the climate model inter-comparison project (CMIP). The ensemble means
 262 are in table 1. Using equation (10) and the estimated parameters, the theoretical change in the net
 263 radiative feedback $\Delta\lambda_t = \lambda_t(150 \text{ yr}) - \lambda_t(1 \text{ yr})$ is calculated. It is compared with the difference in
 264 the slopes obtained from the regressions of N on T from the first twenty years, and from the years
 265 21 to 150. Figure 2 shows that the theoretical expression simulates correctly the change in net
 radiative feedback ($r = 0.93$).

Ensemble	$F / \text{W m}^{-2}$	$C / \text{W yr m}^{-2} \text{K}^{-1}$			$\lambda / \text{W m}^{-2} \text{K}^{-1}$	$\gamma / \text{W m}^{-2} \text{K}^{-1}$	$\hat{\varepsilon} / 1$	$t_{\text{rev}} / \text{yr}$
		C_u	C_d					
CMIP5	7.52	8.53	105.17	-1.21	0.68	1.26	18.53	
CMIP6	7.48	8.06	95.88	-1.02	0.66	1.30	18.31	

254 TABLE 1. CMIP5 and CMIP6 ensemble averages of the thermal and radiative parameters of the modified
 255 linearized two-layer model and estimates of the sign reversal timescale t_{rev} .

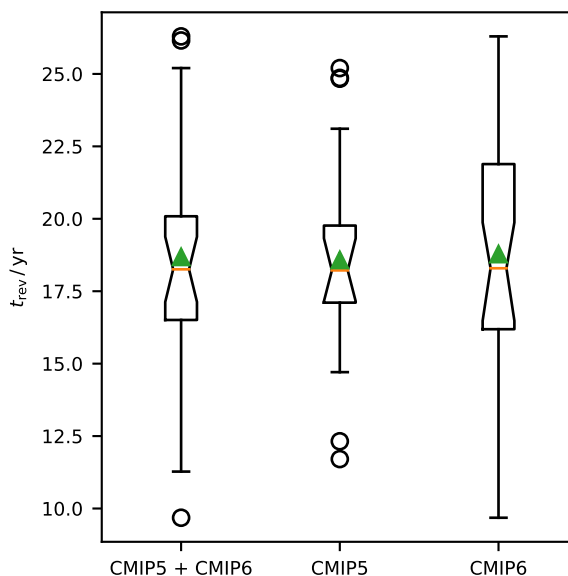
266
 271 Given that t_{rev} provides a new timescale, it probably serves as a justification for how we calculate
 272 the change in the net radiative feedback: the twenty-year timescale used in this study or, e.g., Ceppi
 273 and Gregory (2017). The ensemble means for t_{rev} are consistent: around 18 years for the sign
 274 reversal in either ensemble (Table 1): after 18 years, the $\mathcal{F}_{\text{pat, dyn}}$ term contributes to further the
 275 weakening of the net radiative feedback. In Figure 3, we can see the distribution of t_{rev} in the CMIP



256 FIG. 2. Comparison between the theoretical change in the net radiative feedback and the corresponding from
 257 GCMs. Grey line, the 1-1 line. Black dots, theoretical estimate based in the estimated parameters of the modified
 258 linearized two-layer model versus the change estimated using regression from the NT-diagrams.

276 ensembles. The median is around 18 years and the total range is between 9 and 27 years. Thus, the
 277 twenty-year timescale for studying the net radiative feedback variation has a theoretical support.

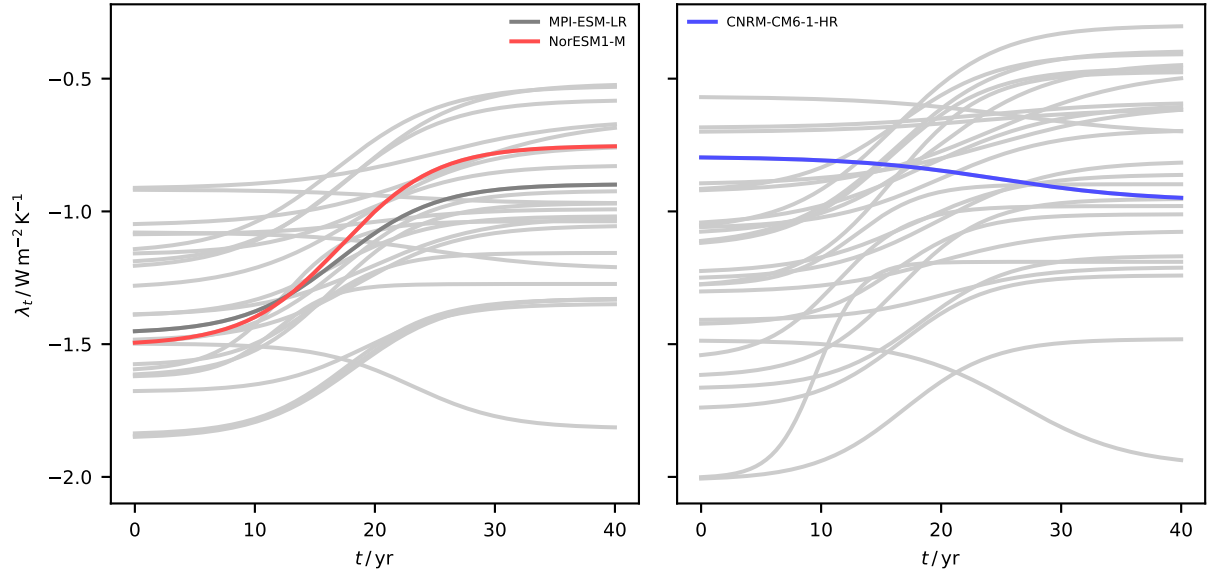
282 We can have a look at the diversity of behaviors in the CMIP ensembles. In Figure 4, I show
 283 all the models' theoretical evolution of the net radiative feedback. The highlighted models are
 284 the ones shown in Figure 1, which shows a model with a strong pattern effect (red), one with a
 285 mild pattern effect (grey), and one with a reversed pattern effect (blue). The CMIP5 ensemble has
 286 less spread in the starting radiative feedback as well as in the late feedback. The CMIP6 case is
 287 more diverse and the late feedbacks are in general more weaker than in the CMIP5 case. Since
 288 the amplitude, time of sign reversal and scaling of the hyperbolic tangent of equation 18 depend
 289 on the estimates of C_u , C_d , λ , γ near the starting state, this can explain this diversity in the CMIP
 290 ensembles. Additionally, one can look here graphically that the time of sign reversal is more or less
 291 constrained in both ensembles, as the mid-point between the early and late feedbacks is attained
 292 near to year 20.



267 FIG. 3. Time of sign reversal in the CMIP ensembles. Each box represents the inter-quartile range of the data.
 268 The orange line is the median and the green triangle shows the mean. The notches on the boxes show the 95
 269 percent confidence interval of the median. The whiskers are at a distance of 1.5 times the inter-quartile range
 270 from the first and third quartile.

293 4. Analysis and Discussion

294 Held et al. (2010) have already proposed that an efficacy in the deep-ocean energy uptake would
 295 be equivalent to changing the thermal capacity of the deep-ocean layer, as Geoffroy et al. (2013a)
 296 also noted. Therefore, my initial discussion of the non-linear planetary energy budget (7) shows
 297 that such an interpretation is more physical than the usual interpretation as a peculiar atmospheric
 298 radiative feedback mechanism. One problem with a thermal-capacity is that we picture Earth's
 299 thermal capacity as the thermal capacity due to all the matter on the Earth system's components.
 300 However, the thermal capacities in equations (7) and (8) are global representations of how the
 301 ocean circulation distributes the energy in the system. After forcing, the ocean circulation changes,
 302 altering the ocean stratification and which parts of the ocean are active at storing energy. This
 303 fact impacts the energy distribution and the efficacy of storing more energy. Consequently, this
 304 evolving energy distribution generates the evolving surface warming pattern. In recent studies, the
 305 role circulation changes in the ocean energy uptake and its effect on the regional warming pattern



278 FIG. 4. Time of sign reversal in the CMIP ensembles. Each box represents the inter-quartile range of the data.
 279 The orange line is the median and the green triangle shows the mean. The notches on the boxes show the 95
 280 percent confidence interval of the median. The whiskers are at a distance of 1.5 times the inter-quartile range
 281 from the first and third quartile.

306 has been uncovered. The southern ocean temperatures are connected with the tropics (Newsom
 307 et al. 2020; Yuan-Jen et al. 2021; Hu et al. 2021). In the southern ocean the complex interactions
 308 between deep-water formation and upwelling shape the long-term ocean overturning circulation
 309 and influence the pacific basin shallower layers (Talley 2015).

310 Apart from the linearization, the two-layer model (8) preserves the traces of this process of
 311 redistributing the energy as shown in the pattern effect contribution to the net radiative feedback
 312 magnitude, equations (13) and (14). This fact further supports the idea that the term $H - H'$ cannot
 313 be interpreted as an atmospheric radiative feedback mechanism. Here, the energy redistribution
 314 is between the upper and deep layers. If the energy distribution is uncoupled ($\hat{\epsilon} = 1$), there will
 315 be no change in the net radiative feedback. One can then ask to formulate the problem in terms
 316 of a two-region model for mimicking the spatial warming pattern directly. Rohrschneider et al.
 317 (2019) demonstrated that two-region models are mathematically equivalent to two-layer models,
 318 further supporting the discussion on how $H - H'$ represents a physical reality and is not only a
 319 mathematical artifice to provide further usability to a broken framework.

320 In the results, I show that the estimates of the thermal, circulation, and radiative parameters have
321 a substantial effect on the evolution of the net radiative feedback. In light of the discussion, partic-
322 ularly the thermal capacities and γ represent an initial energy distribution that evolves depending
323 on the magnitude of $\hat{\epsilon}$. $\hat{\epsilon}$ represents the magnitude of the coupling of the energy distribution and
324 the surface temperature. Therefore, GCMs will show diverse behaviors for the variation of the
325 net radiative feedback as their initial energy uptake and the rate at which it changes with ocean
326 circulation widely varies (Kiehl 2007).

327 In my analysis of the two-layer model, the dependence of the variation of the net radiative feedback
328 with the strength of forcing (Senior and Mitchell 2000; Meraner et al. 2013; Rohrschneider et al.
329 2019) is missing. However, such dependence should come from the values of $\hat{\epsilon}$, λ , γ , and the
330 thermal capacities under a particular forcing and, probably, non-linearity. The thermal capacities,
331 λ , and γ are only approximations of the actual quantities in the neighborhood of the starting states.
332 Therefore, we need a consistent theory on how the different types and magnitudes of forcing modify
333 (a) the coupling between ocean energy distribution and surface temperature, (b) the atmospheric
334 radiative feedback mechanisms, and (c) the rate of energy uptake. Such a theory should describe
335 the Earth system not in the tiny details or as an aggregate of separate disciplines but as an integrated
336 system. The idea can be better expressed as the difference between describing a tree as an aggregate
337 of cells of different types with different functions and describing the whole tree function in terms
338 of certain characteristic variables. In the best case, the needed theory for the climate is incomplete.
339 However, having such a basic conceptual theory of climate will help us better interpret complex
340 model results, find more hidden relationships between important variables and, possibly, reduce
341 the uncertainty in observational estimates of climate sensitivity.

342 **5. Conclusions**

343 In the context of the modified linearized two-layer model (8), I show that variation of net
344 radiative feedback due to the evolving spatial pattern of warming cannot be directly explained
345 by a hidden variable in the atmospheric radiative feedback mechanisms. To show this fact, I
346 discuss how this view is utterly artificial in the context of a global non-linear version of the
347 energy budget (7) and provide an alternative interpretation. This alternative perspective proposes
348 that the thermal capacities used in equations (7) and (8) change, because the ocean circulation

349 changes the distribution of energy in the ocean, the efficacy of the energy uptake and the sea
350 surface temperature. This new perspective is consistent with recent studies (Newsom et al. 2020;
351 Hu et al. 2021; Yuan-Jen et al. 2021). I also present for the first time an explicit mathematical
352 expression of the net radiative feedback in the two-layer model (8) and particularize it for a case
353 of constant forcing. From the analysis, I (a) confirm that the the time-varying term (18) mimics
354 the redistribution of energy between the upper and deep layers, varying the net radiative feedback;
355 and (b) uncover another timescale t_{rev} in the Earth System: the timescale for the change in the net
356 radiative feedback in the abrupt-4xCO2 experiments in GCMs. Using the parameters estimated
357 in the same way as Geoffroy et al. (2013a) did, I find that t_{rev} is around 18 years in CMIP models,
358 providing theoretical support to the 20-year standard timescale used to study the variations in the
359 net radiative feedback in abrupt-4xCO2 experiments. These results motivate us to continue a
360 conceptual characterization of the Earth system. This conceptual theory is necessary to interpret
361 our complex models better, find hidden relationships between variables, or reduce the uncertainty
362 in observationally-based estimates of future climate change.

363 *Acknowledgments.* I thank Hauke Schmidt, Jiawei Bao, Christopher Hedemann and Moritz Gün-
364 ther for reading and correcting the manuscript and for the lively discussions on how to present
365 these highly theoretical ideas.

366 *Data availability statement.* The theoretical considerations are fully described in the appendix of
367 this article. The software to reproduce the numerical results can be found in Jiménez-de-la-Cuesta
368 (2022a). All the post-processed CMIP data is deposited in Jiménez-de-la-Cuesta (2022b).

369 APPENDIX A

370 **Mathematical analysis of the modified two-layer model**

371 In Classical Mechanics, a very coarse thinking would be reducing the field to the task of solving
372 the equation $\dot{\mathbf{p}} = \mathbf{F}$ for any force term, either analytically or numerically. Going further leads to
373 conservation principles and formulations of Classical Mechanics that provide more information
374 without actually obtaining solutions, if that is possible at all. In this appendix, reduced to the scale
375 of a simplified framework, I show that by delving deep into the mathematics of a system of linear

376 ordinary differential equations, the structure of the solutions and its physical interpretation, one
 377 can obtain a new view on an old problem.

378 The appendix is written in an exhaustive way and I leave few things without development. The
 379 cases in which I do not show some algebraic step is because the necessary step has been already
 380 done or is very simple. For simplicity ΔT_u and ΔT_d are always rewritten as T_u and T_d for the
 381 two-layer model.

382 Matrix form of the equations

383 The equations of two-layer model Geoffroy et al. (2013a) are

$$\begin{aligned}
 384 \quad N_u &= C_u \dot{T}_u = F + \lambda T_u - \hat{\varepsilon} \gamma (T_u - T_d) \\
 385 \quad N_d &= C_d \dot{T}_d = \gamma (T_u - T_d)
 \end{aligned} \tag{A1}$$

386 and the planetary imbalance is $N = N_u + N_d$. I present another form of the equations, where I
 387 divide by the thermal capacities.

$$\begin{aligned}
 388 \quad \dot{T}_u &= \frac{F}{C_u} + \frac{\lambda}{C_u} T_u - \hat{\varepsilon} \frac{\gamma}{C_u} (T_u - T_d) \\
 389 \quad \dot{T}_d &= \frac{\gamma}{C_d} (T_u - T_d)
 \end{aligned}$$

390 If I define $F' := F/C_u$, $\lambda' := \lambda/C_u$, $\gamma' := \gamma/C_u$, $\gamma'_d := \gamma/C_d$, one can write the equations in a
 391 lean way

$$\begin{aligned}
 392 \quad \dot{T}_u &= F' + \lambda' T_u - \hat{\varepsilon} \gamma' (T_u - T_d) \\
 393 \quad \dot{T}_d &= \gamma'_d (T_u - T_d)
 \end{aligned} \tag{A2}$$

394 I will put the system in matrix form. I define $\mathbf{T} := (T_u, T_d)$, $\mathbf{F}' := (F', 0)$ and

$$\mathbf{A} := \begin{pmatrix} \lambda' - \hat{\varepsilon} \gamma' & \gamma'_d \\ \hat{\varepsilon} \gamma' & -\gamma'_d \end{pmatrix} \tag{A3}$$

397 and the system can be written

$$\dot{\mathbf{T}} = \mathbf{F}' + \mathbf{T}\mathbf{A} \tag{A4}$$

400 which is the representation of the system in the temperature basis.

401 Eigenvalues and eigenvectors

402 I want to analyse the normal modes of the system. For that end, I need the eigenvalues of the
403 homogeneous system obtained as the solutions of the characteristic equation

$$404 \quad (\lambda' - \hat{\epsilon}\gamma' - \mu)(-\gamma'_d - \mu) - \hat{\epsilon}\gamma'\gamma'_d = 0 \quad (A5)$$

$$407 \quad -\lambda'\gamma'_d + \hat{\epsilon}\gamma'\gamma'_d + \mu\gamma'_d - \lambda'\mu + \hat{\epsilon}\gamma'\mu + \mu^2 - \hat{\epsilon}\gamma'\gamma'_d = 0$$

$$408 \quad -\lambda'\gamma'_d + \mu\gamma'_d - \lambda'\mu + \hat{\epsilon}\gamma'\mu + \mu^2 = 0$$

$$409 \quad -\lambda'\gamma'_d - (\lambda' - \hat{\epsilon}\gamma' - \gamma'_d)\mu + \mu^2 = 0$$

411 The solutions of equation (A5) are

$$412 \quad \mu = \frac{(\lambda' - \hat{\epsilon}\gamma' - \gamma'_d) \pm [(\lambda' - \hat{\epsilon}\gamma' - \gamma'_d)^2 + 4\lambda'\gamma'_d]^{1/2}}{2} \quad (A6)$$

414 and, given that in the Earth $C_u < C_d$, one can prove that there are two real and different eigenval-
415 ues. One needs to check that the square root term is not complex or zero. This only happens if the
416 sum within the square root is negative or zero

$$417 \quad (\lambda' - \hat{\epsilon}\gamma' - \gamma'_d)^2 + 4\lambda'\gamma'_d \leq 0$$

$$418 \quad (\lambda' - \hat{\epsilon}\gamma')^2 - 2(\lambda' - \hat{\epsilon}\gamma')\gamma'_d + \gamma'_d{}^2 + 4\lambda'\gamma'_d \leq 0$$

$$419 \quad \lambda'^2 - 2\lambda'\hat{\epsilon}\gamma' + (\hat{\epsilon}\gamma')^2 - 2(\lambda' - \hat{\epsilon}\gamma')\gamma'_d + \gamma'_d{}^2 + 4\lambda'\gamma'_d \leq 0$$

$$420 \quad \lambda'^2 - 2\lambda'\hat{\epsilon}\gamma' + (\hat{\epsilon}\gamma')^2 - 2\lambda'\gamma'_d + 2\hat{\epsilon}\gamma'\gamma'_d + \gamma'_d{}^2 + 4\lambda'\gamma'_d \leq 0$$

$$421 \quad (\lambda'/\gamma'_d)^2 - 2(\lambda'/\gamma'_d)\hat{\epsilon}(\gamma'/\gamma'_d) + (\hat{\epsilon}(\gamma'/\gamma'_d))^2 + 2\hat{\epsilon}(\gamma'/\gamma'_d) + 1 + 2(\lambda'/\gamma'_d) \leq 0$$

$$422 \quad (\lambda'/\gamma'_d)^2 - 2(\lambda'/\gamma'_d)[\hat{\epsilon}(\gamma'/\gamma'_d) - 1] + (\hat{\epsilon}(\gamma'/\gamma'_d))^2 + 2\hat{\epsilon}(\gamma'/\gamma'_d) + 1 \leq 0$$

$$423 \quad (\lambda'/\gamma'_d)^2 - 2(\lambda'/\gamma'_d)[\hat{\epsilon}(\gamma'/\gamma'_d) - 1] + (\hat{\epsilon}(\gamma'/\gamma'_d) + 1)^2 \leq 0$$

$$424 \quad (\lambda'/\gamma'_d)^2 + (\hat{\epsilon}(C_d/C_u) + 1)^2 \leq 2(\lambda'/\gamma'_d)[\hat{\epsilon}(C_d/C_u) - 1]$$

426 In the last inequality, the left-hand side is always positive. The right-hand side depends on the
 427 sign of the factors. The middle factor is negative since λ' is negative and γ'_d is positive. The third
 428 factor is positive provided that $\hat{\varepsilon} > C_u/C_d$. Given that $\hat{\varepsilon} \geq 1$ and $C_u < C_d$, then the third factor
 429 is positive in our case. Then the right-hand side is negative. Thus, we obtained a contradiction
 430 by supposing that the square root term was negative or zero. Therefore, the conclusion is that
 431 the eigenvalues are two real and distinct numbers. Some CMIP5 models show $\hat{\varepsilon} < 1$ according
 432 to Geoffroy et al. (2013a). These also fit here. In the last condition of the above expression we
 433 require that $\hat{\varepsilon}(C_d/C_u) - 1 > 0$. If $\hat{\varepsilon} \geq C_u/C_d$ this is fulfilled. C_u/C_d is a small quantity and, in the
 434 models that have a lesser than one $\hat{\varepsilon}$, always the $\hat{\varepsilon}$ is larger than this small quantity by an order of
 435 magnitude. Thus, what I had said until now and will be said afterwards applies to all cases.

436 I call the solutions μ_+ and μ_- , depending on the sign of the square root term. Let us rewrite their
 437 expression in more lean fashion. I define $\hat{\lambda} := \lambda' - \hat{\varepsilon}\gamma' - \gamma'_d$ and we call κ the square root term.
 438 Then, I rewrite the solutions (A6) as

$$439 \mu_{\pm} = \frac{\hat{\lambda} \pm \kappa}{2} \quad (A7)$$

441 Now that I know the eigenvalues, one should get the eigenvectors of the system and solve it
 442 easily. The eigenvectors are the generators of the kernel of the operators $\mathbf{A} - \mu_{\pm} \text{id}$. Let us write
 443 the diagonal of the matrix \mathbf{A} with the definition of $\hat{\lambda}$

$$444 \mathbf{A} = \begin{pmatrix} \hat{\lambda} + \gamma'_d & \gamma'_d \\ \hat{\varepsilon}\gamma' & \hat{\lambda} - (\lambda' - \hat{\varepsilon}\gamma') \end{pmatrix}$$

446 and then the matrices for each eigenvalue have the form

$$447 \mathbf{A} - \mu_{\pm} \text{id} = \begin{pmatrix} \hat{\lambda} + \gamma'_d - \mu_{\pm} & \gamma'_d \\ \hat{\varepsilon}\gamma' & \hat{\lambda} - (\lambda' - \hat{\varepsilon}\gamma') - \mu_{\pm} \end{pmatrix}$$

$$448 = \begin{pmatrix} \mu_{\mp} + \gamma'_d & \gamma'_d \\ \hat{\varepsilon}\gamma' & \mu_{\mp} - (\lambda' - \hat{\varepsilon}\gamma') \end{pmatrix}$$

450 Since eigenvalues are real and distinct, there should be two linearly-independent eigenvectors,
 451 one for each eigenvalue. These vectors should fulfill that $\mathbf{e}_{\pm}(\mathbf{A} - \mu_{\pm} \text{id}) = 0$. Solving that linear

452 system, I find the eigenvectors in temperature representation

$$453 \quad \mathbf{e}_{\pm} = \mathbf{e}_u - \frac{\mu_{\mp} + \gamma'_d}{\hat{\varepsilon}\gamma'} \mathbf{e}_d \quad (A8)$$

454

455 The procedure to get the result is to solve the system of homogeneous linear equations $\mathbf{e}_{\pm}(\mathbf{A} -$
 456 $\mu_{\pm} \text{id}) = 0$

$$457 \quad \begin{cases} (\mu_{\mp} + \gamma'_d)e_{\pm,u} & + \hat{\varepsilon}\gamma' e_{\pm,d} = 0 \\ \gamma'_d e_{\pm,u} + [\mu_{\mp} - (\lambda' - \hat{\varepsilon}\gamma')]e_{\pm,d} = 0 \end{cases}$$

458

459 I solve the first equation for the component $e_{\pm,d}$, and substitute this result on the second equation

$$460 \quad e_{\pm,d} = -\frac{\mu_{\mp} + \gamma'_d}{\hat{\varepsilon}\gamma'} e_{\pm,u} \longrightarrow$$

$$461 \quad \left(\gamma'_d - \frac{[\mu_{\mp} - (\lambda' - \hat{\varepsilon}\gamma')](\mu_{\mp} + \gamma'_d)}{\hat{\varepsilon}\gamma'} \right) e_{\pm,u} = 0$$

$$462 \quad \frac{\hat{\varepsilon}\gamma'\gamma'_d - [\mu_{\mp} - (\lambda' - \hat{\varepsilon}\gamma')](\mu_{\mp} + \gamma'_d)}{\hat{\varepsilon}\gamma'} e_{\pm,u} = 0, (\hat{\varepsilon}, \gamma' \neq 0) \therefore$$

463

464

$$465 \quad \{ \hat{\varepsilon}\gamma'\gamma'_d - [\mu_{\mp} - (\lambda' - \hat{\varepsilon}\gamma')](\mu_{\mp} + \gamma'_d) \} e_{\pm,u} = 0$$

$$466 \quad \{ \hat{\varepsilon}\gamma'\gamma'_d + [(\lambda' - \hat{\varepsilon}\gamma') - \mu_{\mp}](\gamma'_d + \mu_{\mp}) \} e_{\pm,u} = 0$$

$$467 \quad - \{ -\hat{\varepsilon}\gamma'\gamma'_d + [(\lambda' - \hat{\varepsilon}\gamma') - \mu_{\mp}](-\gamma'_d - \mu_{\mp}) \} e_{\pm,u} = 0$$

468

469 and in the last expression we have two options: either $e_{\pm,u}$ is zero or the term within curly braces is
 470 zero. However, the expression in curly braces is the characteristic equation (A5) and then always
 471 vanishes identically. This means that $e_{\pm,u} = \alpha \in \mathbb{R}$ can be chosen arbitrarily. I plug in this result
 472 in the expression for $e_{\pm,d}$ and get that

$$473 \quad e_{\pm,u} = \alpha$$

$$474 \quad e_{\pm,d} = -\frac{\mu_{\mp} + \gamma'_d}{\hat{\varepsilon}\gamma'} \alpha$$

475

476 or as a vector in the temperature basis

$$477 \quad \mathbf{e}_{\pm} = e_{\pm,u} \mathbf{e}_u + e_{\pm,d} \mathbf{e}_d$$

$$478 \quad \mathbf{e}_{\pm} = \alpha \mathbf{e}_u - \frac{\mu_{\mp} + \gamma'_d}{\hat{\epsilon} \gamma'} \alpha \mathbf{e}_d$$

479

480 and since α is arbitrary this means we are in front of a subspace of vectors. I choose a basis by
481 selecting $\alpha = 1$.

$$482 \quad \mathbf{e}_{\pm} = \mathbf{e}_u - \frac{\mu_{\mp} + \gamma'_d}{\hat{\epsilon} \gamma'} \mathbf{e}_d$$

483

484 which is the same as the equation (A8).

485 Now, I can derive the expressions of the temperature basis vectors in terms of the two eigenvectors.

486 If one solves for e_u in equation (A8)

$$487 \quad \mathbf{e}_{\pm} + \frac{\mu_{\mp} + \gamma'_d}{\hat{\epsilon} \gamma'} \mathbf{e}_d = \mathbf{e}_u$$

488

489 but we have here two expressions in a condensed way. Therefore,

$$490 \quad \mathbf{e}_- + \frac{\mu_+ + \gamma'_d}{\hat{\epsilon} \gamma'} \mathbf{e}_d = \mathbf{e}_+ + \frac{\mu_- + \gamma'_d}{\hat{\epsilon} \gamma'} \mathbf{e}_d$$

$$491 \quad \left(\frac{\mu_+ + \gamma'_d}{\hat{\epsilon} \gamma'} - \frac{\mu_- + \gamma'_d}{\hat{\epsilon} \gamma'} \right) \mathbf{e}_d = \mathbf{e}_+ - \mathbf{e}_-$$

$$492 \quad \frac{(\mu_+ + \gamma'_d) - (\mu_- + \gamma'_d)}{\hat{\epsilon} \gamma'} \mathbf{e}_d = \mathbf{e}_+ - \mathbf{e}_-$$

$$493 \quad \frac{\mu_+ - \mu_-}{\hat{\epsilon} \gamma'} \mathbf{e}_d = \mathbf{e}_+ - \mathbf{e}_-$$

$$494 \quad \mathbf{e}_d = \frac{\hat{\epsilon} \gamma'}{\mu_+ - \mu_-} (\mathbf{e}_+ - \mathbf{e}_-)$$

495

496 Thus, I have expressed \mathbf{e}_d in terms of the eigenvectors.

497 Now, I substitute the last result on one of the expressions for \mathbf{e}_u .

$$498 \quad \mathbf{e}_+ + \frac{\mu_- + \gamma'_d}{\hat{\epsilon}\gamma'} \mathbf{e}_d = \mathbf{e}_u$$

$$499 \quad \mathbf{e}_+ + \frac{\mu_- + \gamma'_d}{\hat{\epsilon}\gamma'} \frac{\hat{\epsilon}\gamma'}{\mu_+ - \mu_-} (\mathbf{e}_+ - \mathbf{e}_-) = \mathbf{e}_u$$

$$500 \quad \mathbf{e}_+ + \frac{\mu_- + \gamma'_d}{\mu_+ - \mu_-} (\mathbf{e}_+ - \mathbf{e}_-) = \mathbf{e}_u$$

$$501 \quad \left(1 + \frac{\mu_- + \gamma'_d}{\mu_+ - \mu_-}\right) \mathbf{e}_+ - \frac{\mu_- + \gamma'_d}{\mu_+ - \mu_-} \mathbf{e}_- = \mathbf{e}_u$$

$$502 \quad \frac{\mu_+ - \mu_- + \mu_- + \gamma'_d}{\mu_+ - \mu_-} \mathbf{e}_+ - \frac{\mu_- + \gamma'_d}{\mu_+ - \mu_-} \mathbf{e}_- = \mathbf{e}_u$$

$$503 \quad \frac{\mu_+ + \gamma'_d}{\mu_+ - \mu_-} \mathbf{e}_+ - \frac{\mu_- + \gamma'_d}{\mu_+ - \mu_-} \mathbf{e}_- = \mathbf{e}_u$$

504

505 and the temperature basis vectors in the eigenvector representation are

$$506 \quad \mathbf{e}_u = \frac{\mu_+ + \gamma'_d}{\mu_+ - \mu_-} \mathbf{e}_+ - \frac{\mu_- + \gamma'_d}{\mu_+ - \mu_-} \mathbf{e}_- \quad (\text{A9})$$

$$507 \quad \mathbf{e}_d = \frac{\hat{\epsilon}\gamma'}{\mu_+ - \mu_-} (\mathbf{e}_+ - \mathbf{e}_-)$$

508 **Matrix in the eigenvector representation. Solutions**

509 With these results, I can write the matrix \mathbf{A} (A3) in the eigenvector basis and it should be the
510 following diagonal matrix

$$511 \quad \mathbf{B} = \begin{pmatrix} \mu_+ & 0 \\ 0 & \mu_- \end{pmatrix} \quad (\text{A10})$$

513 I show how to get to this result. Let subscripts represent rows and superscripts represent columns.

514 I define that latin indices (i, j, k, \dots) have the possible values u, d; and greek indices ($\alpha, \beta, \zeta \dots$)

515 have possible values +, -. Also, repeated indices in expressions mean summation over the set of

516 possible values. With these considerations, equation (A9) is

$$517 \quad \mathbf{e}_i = \Lambda_i^\alpha \mathbf{e}_\alpha$$

518

519 where the rows of matrix Λ contain the coordinates of each of the vectors of the temperature basis
520 in the eigenvector representation. Analogously, equation (A8) is

$$521 \quad \mathbf{e}_\alpha = \Theta_\alpha^i \mathbf{e}_i$$

522

523 where matrix Θ has in its rows the coordinates the eigenvector basis in the temperature represen-
524 tation. This means that

$$525 \quad \mathbf{e}_\alpha = \Theta_\alpha^i \mathbf{e}_i = \Theta_\alpha^i \Lambda_i^\beta \mathbf{e}_\beta$$

526

527 which is only possible if the matrices Λ and Θ are inverse of each other

$$528 \quad \mathbf{e}_\alpha = \delta_\alpha^\beta \mathbf{e}_\beta = \mathbf{e}_\alpha$$

529

530 Thus, we write $\Theta = \Lambda^{-1}$.

531 Now, matrix \mathbf{A} is the temperature representation of a linear operator f . If $\mathbf{v} = v^j \mathbf{e}_j$ is a vector in
532 the temperature representation, then the action of the linear operator f should be $f(\mathbf{v}) = f(v^j \mathbf{e}_j) =$
533 $v^j f(\mathbf{e}_j)$. Then the action of f on a vector expressed in a given basis only depends on the action
534 of the operator on the basis: $f(\mathbf{v}) = f(v^j \mathbf{e}_j) = v^j f(\mathbf{e}_j) = v^j \mathbf{A}_j^k \mathbf{e}_k$. Thus, the matrix \mathbf{A} has in its
535 rows the coordinates in the temperature representation of the action of f over each basis vector.
536 Once one understands what is happening under the hood, what we want is the matrix \mathbf{B} , which
537 is the representation of f in the eigenvector basis. Therefore, I begin with the basic relationship
538 in the temperature representation and introduce the change of representation using the alternative

539 representation of equations (A8) and (A9)

$$\begin{aligned}
540 \quad & f(\mathbf{e}_i) = \mathbf{A}_i^j \Lambda_j^\zeta \mathbf{e}_\zeta \\
541 \quad & f(\Lambda_i^\alpha \mathbf{e}_\alpha) = \mathbf{A}_i^j \Lambda_j^\zeta \mathbf{e}_\zeta \\
542 \quad & \Lambda_i^\alpha f(\mathbf{e}_\alpha) = \mathbf{A}_i^j \Lambda_j^\zeta \mathbf{e}_\zeta \\
543 \quad & (\Lambda^{-1})_\beta^i \Lambda_i^\alpha f(\mathbf{e}_\alpha) = (\Lambda^{-1})_\beta^i \mathbf{A}_i^j \Lambda_j^\zeta \mathbf{e}_\zeta \\
544 \quad & f(\mathbf{e}_\beta) = (\Lambda^{-1})_\beta^i \mathbf{A}_i^j \Lambda_j^\zeta \mathbf{e}_\zeta, f(\mathbf{e}_\beta) := \mathbf{B}_\beta^\zeta \mathbf{e}_\zeta \\
545 \quad & \mathbf{B}_\beta^\zeta = (\Lambda^{-1})_\beta^i \mathbf{A}_i^j \Lambda_j^\zeta \\
546
\end{aligned}$$

547 or in matrix notation $\mathbf{B} = \Lambda^{-1} \mathbf{A} \Lambda$. Then, I multiply the matrices

$$\begin{aligned}
548 \quad & \Lambda^{-1} = \begin{pmatrix} 1 & -\frac{\mu_- + \gamma'_d}{\hat{\varepsilon} \gamma'} \\ 1 & -\frac{\mu_+ + \gamma'_d}{\hat{\varepsilon} \gamma'} \end{pmatrix}, \mathbf{A} = \begin{pmatrix} \hat{\lambda} + \gamma'_d & \gamma'_d \\ \hat{\varepsilon} \gamma' & -\gamma'_d \end{pmatrix}, \Lambda = \begin{pmatrix} \frac{\mu_+ + \gamma'_d}{\mu_+ - \mu_-} & -\frac{\mu_- + \gamma'_d}{\mu_+ - \mu_-} \\ \frac{\hat{\varepsilon} \gamma'}{\mu_+ - \mu_-} & -\frac{\hat{\varepsilon} \gamma'}{\mu_+ - \mu_-} \end{pmatrix} \\
549
\end{aligned}$$

550 First, note that $\mu_+ - \mu_- = \kappa$. One also looks at the following quantities that will help in the
551 process: $\mu_+ + \mu_- = \hat{\lambda}$ and $\mu_+ \mu_- = \frac{1}{4}(\hat{\lambda}^2 - \kappa^2) = \frac{1}{4}(\hat{\lambda}^2 - \hat{\lambda}^2 - 4\lambda' \gamma'_d) = -\lambda' \gamma'_d$. I proceed with the
552 first product, $\Lambda^{-1} \mathbf{A}$.

$$\begin{aligned}
553 \quad & \Lambda^{-1} \mathbf{A} = \begin{pmatrix} 1 & -\frac{\mu_- + \gamma'_d}{\hat{\varepsilon} \gamma'} \\ 1 & -\frac{\mu_+ + \gamma'_d}{\hat{\varepsilon} \gamma'} \end{pmatrix} \begin{pmatrix} \hat{\lambda} + \gamma'_d & \gamma'_d \\ \hat{\varepsilon} \gamma' & -\gamma'_d \end{pmatrix} \\
554 \quad & = \begin{pmatrix} \hat{\lambda} + \gamma'_d - \mu_- - \gamma'_d & \left(1 + \frac{\mu_- + \gamma'_d}{\hat{\varepsilon} \gamma'}\right) \gamma'_d \\ \hat{\lambda} + \gamma'_d - \mu_+ - \gamma'_d & \left(1 + \frac{\mu_+ + \gamma'_d}{\hat{\varepsilon} \gamma'}\right) \gamma'_d \end{pmatrix} \\
555 \quad & = \begin{pmatrix} \hat{\lambda} - \mu_- & \frac{\hat{\varepsilon} \gamma' + \mu_- + \gamma'_d}{\hat{\varepsilon} \gamma'} \gamma'_d \\ \hat{\lambda} - \mu_+ & \frac{\hat{\varepsilon} \gamma' + \mu_+ + \gamma'_d}{\hat{\varepsilon} \gamma'} \gamma'_d \end{pmatrix} \\
556 \quad & = \begin{pmatrix} \mu_+ & \frac{\hat{\varepsilon} \gamma' + \mu_- + \gamma'_d}{\hat{\varepsilon} \gamma'} \gamma'_d \\ \mu_- & \frac{\hat{\varepsilon} \gamma' + \mu_+ + \gamma'_d}{\hat{\varepsilon} \gamma'} \gamma'_d \end{pmatrix} \\
557
\end{aligned}$$

558 and multiply the result by Λ

$$\begin{aligned}
559 \quad \Lambda^{-1} \mathbf{A} \Lambda &= \begin{pmatrix} \mu_+ & \frac{\hat{\varepsilon} \gamma' + \mu_- + \gamma'_d}{\hat{\varepsilon} \gamma'} \gamma'_d \\ \mu_- & \frac{\hat{\varepsilon} \gamma' + \mu_+ + \gamma'_d}{\hat{\varepsilon} \gamma'} \gamma'_d \end{pmatrix} \begin{pmatrix} \frac{\mu_+ + \gamma'_d}{\mu_+ - \mu_-} & -\frac{\mu_- + \gamma'_d}{\mu_+ - \mu_-} \\ \frac{\hat{\varepsilon} \gamma'}{\mu_+ - \mu_-} & -\frac{\hat{\varepsilon} \gamma'}{\mu_+ - \mu_-} \end{pmatrix} \\
560 &= \frac{1}{\kappa} \begin{pmatrix} \mu_+^2 + \mu_+ \gamma'_d + \hat{\varepsilon} \gamma' \gamma'_d + \mu_- \gamma'_d + \gamma'_d{}^2 & -\mu_+ \mu_- - \mu_+ \gamma'_d - \hat{\varepsilon} \gamma' \gamma'_d - \mu_- \gamma'_d - \gamma'_d{}^2 \\ \mu_- \mu_+ + \mu_- \gamma'_d + \hat{\varepsilon} \gamma' \gamma'_d + \mu_+ \gamma'_d + \gamma'_d{}^2 & -\mu_-^2 - \mu_- \gamma'_d - \hat{\varepsilon} \gamma' \gamma'_d - \mu_+ \gamma'_d - \gamma'_d{}^2 \end{pmatrix} \\
561 &= \frac{1}{\kappa} \begin{pmatrix} \mu_+^2 + (\hat{\lambda} + \hat{\varepsilon} \gamma' + \gamma'_d) \gamma'_d & -\mu_+ \mu_- - (\hat{\lambda} + \hat{\varepsilon} \gamma' + \gamma'_d) \gamma'_d \\ \mu_- \mu_+ + (\hat{\lambda} + \hat{\varepsilon} \gamma' + \gamma'_d) \gamma'_d & -\mu_-^2 - (\hat{\lambda} + \hat{\varepsilon} \gamma' + \gamma'_d) \gamma'_d \end{pmatrix} \\
562 &= \frac{1}{\kappa} \begin{pmatrix} \mu_+^2 - \mu_+ \mu_- & \lambda' \gamma'_d - \lambda' \gamma'_d \\ -\lambda' \gamma'_d + \lambda' \gamma'_d & -\mu_-^2 + \mu_+ \mu_- \end{pmatrix} = \frac{1}{\kappa} \begin{pmatrix} \mu_+ \kappa & 0 \\ 0 & \mu_- \kappa \end{pmatrix} = \begin{pmatrix} \mu_+ & 0 \\ 0 & \mu_- \end{pmatrix} \\
563
\end{aligned}$$

564 the last line is the result that we wanted to check.

565 In the eigenvector representation the system (A4) has the following form

$$566 \quad \dot{\mathbf{T}} = \mathbf{F}' + \mathbf{T} \mathbf{B} \quad (\text{A11})$$

568 and, therefore, is decoupled. Therefore, I can solve each equation separately. I only need to
569 transform the forcing vector to the eigenvector representation.

570 The equations are

$$571 \quad \dot{T}_{\pm} = F'_{\pm} + \mu_{\pm} T_{\pm}$$

573 and the solutions of a generic initial value problem are

$$574 \quad T_{\pm} = \left(T_{\pm,0} + \int_{t_0}^t F'_{\pm} e^{-\mu_{\pm}(\tau-t_0)} d\tau \right) e^{\mu_{\pm}(t-t_0)} \quad (\text{A12})$$

576 where the initial values in the eigenvector representation in terms of the initial values in the
577 temperature representation are

$$578 \quad T_{\pm,0} = \pm \frac{1}{\mu_+ - \mu_-} [(\mu_{\pm} + \gamma'_d) T_{u,0} + \hat{\varepsilon} \gamma' T_{d,0}]$$

580 the forcing components are

$$581 \quad F'_{\pm} = \pm \frac{\mu_{\pm} + \gamma'_d}{\mu_+ - \mu_-} F'$$

583 and the solutions in the temperature representation are

$$584 \quad T_u = T_+ + T_-$$

$$585 \quad T_d = -\frac{\mu_- + \gamma'_d}{\hat{\epsilon}\gamma'} T_+ - \frac{\mu_+ + \gamma'_d}{\hat{\epsilon}\gamma'} T_-$$

586 If I further expand the T_d solution, the form of the solutions is more elegant

$$587 \quad T_u = T_+ + T_- \tag{A13}$$

$$588 \quad T_d = -\frac{\hat{\lambda} + 2\gamma'_d}{2\hat{\epsilon}\gamma'} (T_+ + T_-) + \frac{\kappa}{2\hat{\epsilon}\gamma'} (T_+ - T_-)$$

589 since it shows that the solutions in the temperature space are in a sort of symmetric and antisymmet-
 590 ric combinations of the solutions in the eigenvector representation. These are the normal modes.
 591 One thing to note is that the upper temperature is the symmetric mode and the deep temperature is
 592 a mixture of symmetric and antisymmetric modes.

593 I show how I got the solutions (A13). Just expand the T_d equation.

$$594 \quad T_d = -\frac{\mu_- + \gamma'_d}{\hat{\epsilon}\gamma'} T_+ - \frac{\mu_+ + \gamma'_d}{\hat{\epsilon}\gamma'} T_-$$

$$595 \quad = -\frac{1}{\hat{\epsilon}\gamma'} \left[\left(\frac{\hat{\lambda} - \kappa}{2} + \gamma'_d \right) T_+ + \left(\frac{\hat{\lambda} + \kappa}{2} + \gamma'_d \right) T_- \right]$$

$$596 \quad = -\frac{1}{\hat{\epsilon}\gamma'} \left[\left(\frac{\hat{\lambda} + 2\gamma'_d}{2} - \frac{\kappa}{2} \right) T_+ + \left(\frac{\hat{\lambda} + 2\gamma'_d}{2} + \frac{\kappa}{2} \right) T_- \right]$$

$$597 \quad = -\frac{1}{2\hat{\epsilon}\gamma'} \left[(\hat{\lambda} + 2\gamma'_d)(T_+ + T_-) - \kappa(T_+ - T_-) \right]$$

599 From now on, I write $T_s := T_+ + T_-$ and $T_a := T_+ - T_-$.

600 **Planetary imbalance**

601 Now, I will find an expression for the planetary imbalance in terms of the equations (A13). The
 602 mathematical expression that I should expand is $N = N_u + N_d = C_u \dot{T}_u + C_d \dot{T}_d$

$$\begin{aligned}
 603 \quad C_u \dot{T}_u &= C_u \dot{T}_s \\
 604 \quad C_d \dot{T}_d &= -C_d \frac{\hat{\lambda} + 2\gamma'_d}{2\hat{\epsilon}\gamma'} \dot{T}_s + C_d \frac{\kappa}{2\hat{\epsilon}\gamma'} \dot{T}_a \therefore \\
 605 \quad N &= C_u \dot{T}_s - C_d \frac{\hat{\lambda} + 2\gamma'_d}{2\hat{\epsilon}\gamma'} \dot{T}_s + C_d \frac{\kappa}{2\hat{\epsilon}\gamma'} \dot{T}_a \\
 606 \quad &= \left(C_u - C_d \frac{\hat{\lambda} + 2\gamma'_d}{2\hat{\epsilon}\gamma'} \right) \dot{T}_s + C_d \frac{\kappa}{2\hat{\epsilon}\gamma'} \dot{T}_a \\
 607 \quad &= C_s \dot{T}_s + C_a \dot{T}_a \\
 608
 \end{aligned}$$

609 Now, $\dot{T}_\pm = F'_\pm + \mu_\pm T_\pm$, then

$$\begin{aligned}
 610 \quad \dot{T}_s &= \mu_+ T_+ + \mu_- T_- + (F'_+ + F'_-) = \mu_+ T_+ + (\mu_+ - \kappa) T_- + (F'_+ + F'_-) \\
 611 \quad &= \mu_+ T_s - \kappa T_- + (F'_+ + F'_-) = \mu_+ T_s - \frac{\kappa}{2} (T_s - T_a) + (F'_+ + F'_-) \\
 612 \quad &= \frac{\hat{\lambda}}{2} T_s + \frac{\kappa}{2} T_a + (F'_+ + F'_-) = \frac{\hat{\lambda}}{2} T_s + \frac{\kappa}{2} T_a + F' \\
 613 \quad \dot{T}_a &= \mu_+ T_+ - \mu_- T_- + (F'_+ - F'_-) = \mu_+ T_+ - (\mu_+ - \kappa) T_- + (F'_+ - F'_-) \\
 614 \quad &= \mu_+ T_a + \kappa T_- + (F'_+ - F'_-) = \mu_+ T_a + \frac{\kappa}{2} (T_s - T_a) + (F'_+ - F'_-) \\
 615 \quad &= \frac{\kappa}{2} T_s + \frac{\hat{\lambda}}{2} T_a + (F'_+ - F'_-) = \frac{\kappa}{2} T_s + \frac{\hat{\lambda}}{2} T_a + \frac{\hat{\lambda} + 2\gamma'_d}{\kappa} F' \therefore \\
 616 \quad N &= \frac{1}{2} (\hat{\lambda} C_s + \kappa C_a) T_s + \frac{1}{2} (\hat{\lambda} C_a + \kappa C_s) T_a + \left(C_s + C_a \frac{\hat{\lambda} + 2\gamma'_d}{\kappa} \right) F' \\
 617
 \end{aligned}$$

618 Further expanding the coefficients

$$\begin{aligned}
619 \quad \hat{\lambda}C_s + \kappa C_a &= \hat{\lambda}C_u - \frac{C_d}{2\hat{\epsilon}\gamma'}(\hat{\lambda}^2 + 2\gamma'_d\hat{\lambda} - \kappa^2) = \hat{\lambda}C_u - \frac{C_d}{2\hat{\epsilon}\gamma'}(\hat{\lambda}^2 + 2\gamma'_d\hat{\lambda} - \hat{\lambda}^2 - 4\gamma'_d\lambda') \\
620 \quad &= 2\frac{C_u}{\hat{\epsilon}}\left(\lambda' + \frac{\hat{\epsilon} - 1}{2}\hat{\lambda}\right) \\
621 \quad \hat{\lambda}C_a + \kappa C_s &= \kappa C_u - \frac{C_d}{2\hat{\epsilon}\gamma'}(\kappa\hat{\lambda} + 2\gamma'_d\kappa - \kappa\hat{\lambda}) = \kappa C_u - \frac{C_u}{\hat{\epsilon}}\kappa = \kappa\frac{C_u}{\hat{\epsilon}}(\hat{\epsilon} - 1) \\
622 \quad C_s + C_a\frac{\hat{\lambda} + 2\gamma'_d}{\kappa} &= C_u - \frac{C_d}{2\hat{\epsilon}\gamma'}(\hat{\lambda} + 2\gamma'_d - \hat{\lambda} - 2\gamma'_d) = C_u \\
623
\end{aligned}$$

624 then the imbalance is

$$625 \quad N = \frac{C_u}{\hat{\epsilon}}\left[\hat{\epsilon}F' + \left(\lambda' + \frac{\hat{\epsilon} - 1}{2}\hat{\lambda}\right)T_s + \kappa\frac{\hat{\epsilon} - 1}{2}T_a\right] \quad (A14)$$

627 From here, I derive the slope of a NT -diagram. In such a diagram, N is plotted versus T_u . If we
628 naïvely take the partial derivative of equation (A14) with respect to T_u , we will arrive to a constant
629 slope. This is contrary to the evidence that it will change with time. An NT -diagram is one
630 projection of the phase space of the system. Then, the NT -diagram slope does not only depend on
631 how N varies with T_u . It is a comparison of how the changes of T_u are expressed in changes of N .
632 Then, the slope is the total derivative dN/dT_u . By virtue of the chain rule, $dN/dT_u = \dot{N}(dt/dT_u)$.
633 In a neighborhood where $T_u(t)$ is injective, $dt/dT_u = 1/\dot{T}_u$. Therefore, the slope dN/dT_u is the ratio
634 of two total derivatives: \dot{N} and \dot{T}_u .

635 We know that $T_u = T_s$, then $\dot{T}_u = \dot{T}_s$. Therefore, the total derivative of the planetary imbalance is

$$636 \quad \dot{N} = (\partial_t N) + (\partial_{T_s} N)\dot{T}_s + (\partial_{T_a} N)\dot{T}_a$$

638 that is a change depending only on time, a second change depending only on changes of T_s and a
639 third depending on changes of T_a . Therefore, the ratio of total derivative of planetary imbalance
640 and total derivative of T_u is

$$641 \quad \frac{\dot{N}}{\dot{T}_u} = (\partial_t N)\frac{1}{\dot{T}_s} + (\partial_{T_s} N) + (\partial_{T_a} N)\frac{\dot{T}_a}{\dot{T}_s}$$

643 As one can see in the above expression, the ratio includes the derivative of the imbalance with
644 respect to T_u but is not the only contribution. One contribution comes from the explicit dependence
645 on time of N and how it compares with the dependency of T_u . The other contribution comes
646 from the antisymmetric mode and how it changes in relation to the symmetric one. From equation
647 (A14), I can write the precise expression of the slope as a factor of λ .

648 I multiply equation (A14) by λ/λ and reorganise.

$$\begin{aligned}
649 \quad \frac{\dot{N}}{\dot{T}_u} &= \frac{C_u}{\hat{\varepsilon}} \left[\hat{\varepsilon} \frac{\dot{F}'}{\dot{T}_s} + \left(\lambda' + \frac{\hat{\varepsilon} - 1}{2} \hat{\lambda} \right) + \kappa \frac{\hat{\varepsilon} - 1}{2} \frac{\dot{T}_a}{\dot{T}_s} \right] \frac{\lambda}{\lambda} \\
650 \quad &= \left[\frac{C_u}{\lambda} \frac{\dot{F}'}{\dot{T}_s} + \left(\frac{\lambda'}{\hat{\varepsilon} \lambda} + \frac{\hat{\varepsilon} - 1}{2 \hat{\varepsilon}} \frac{\hat{\lambda}}{\lambda'} \right) + \frac{\hat{\varepsilon} - 1}{2 \hat{\varepsilon}} \frac{\kappa}{\lambda'} \frac{\dot{T}_a}{\dot{T}_s} \right] \lambda
\end{aligned}$$

652 then we will expand the terms to separate the terms that vanish when $\hat{\varepsilon} = 1$

$$\begin{aligned}
653 \quad \frac{\dot{N}}{\dot{T}_u} &= \left\{ \frac{C_u}{\lambda} \frac{\dot{F}'}{\dot{T}_s} + \left[\frac{1}{\hat{\varepsilon}} + \frac{\hat{\varepsilon} - 1}{2 \hat{\varepsilon}} \left(\frac{\lambda' - \hat{\varepsilon} \gamma' - \gamma'_d}{\lambda'} \right) \right] + \frac{\hat{\varepsilon} - 1}{2 \hat{\varepsilon}} \frac{\kappa}{\lambda'} \frac{\dot{T}_a}{\dot{T}_s} \right\} \lambda \\
654 \quad &= \left\{ \frac{C_u}{\lambda} \frac{\dot{F}'}{\dot{T}_s} + \left[\frac{2}{2 \hat{\varepsilon}} + \frac{\hat{\varepsilon} - 1}{2 \hat{\varepsilon}} \left(1 - \hat{\varepsilon} \frac{\gamma}{\lambda} - \frac{C_u \gamma}{C_d \lambda} \right) \right] + \frac{\hat{\varepsilon} - 1}{2 \hat{\varepsilon}} \frac{C_u \kappa}{\lambda} \frac{\dot{T}_a}{\dot{T}_s} \right\} \lambda \\
655 \quad &= \left[\frac{C_u}{\lambda} \frac{\dot{F}'}{\dot{T}_s} + \frac{\hat{\varepsilon} + 1}{2 \hat{\varepsilon}} - \frac{\hat{\varepsilon} - 1}{2 \hat{\varepsilon}} \left(\hat{\varepsilon} + \frac{C_u}{C_d} \right) \frac{\gamma}{\lambda} + \frac{\hat{\varepsilon} - 1}{2 \hat{\varepsilon}} \frac{C_u \kappa}{\lambda} \frac{\dot{T}_a}{\dot{T}_s} \right] \lambda \\
656 \quad &= \left[\frac{C_u}{\lambda} \frac{\dot{F}'}{\dot{T}_s} + \frac{\hat{\varepsilon} + 1}{2 \hat{\varepsilon}} - \frac{\hat{\varepsilon} - 1}{2 \hat{\varepsilon}} \left(\hat{\varepsilon} + \frac{C_u}{C_d} \right) \frac{\gamma}{\lambda} + \frac{\hat{\varepsilon} - 1}{2 \hat{\varepsilon}} \frac{C_u \kappa}{\lambda} \frac{\dot{T}_a}{\dot{T}_s} \right] \lambda \\
657 \quad &= \left\{ \frac{C_u}{\lambda} \frac{\dot{F}'}{\dot{T}_s} + \frac{\hat{\varepsilon} + 1}{2 \hat{\varepsilon}} - \frac{\hat{\varepsilon} - 1}{2 \hat{\varepsilon} \lambda} \left[\left(\hat{\varepsilon} + \frac{C_u}{C_d} \right) \gamma - C_u \kappa \frac{\dot{T}_a}{\dot{T}_s} \right] \right\} \lambda \\
658 \quad &= \left\{ \frac{C_u}{\lambda} \frac{\dot{F}'}{\dot{T}_s} + \frac{\hat{\varepsilon} + 1}{2 \hat{\varepsilon}} - \frac{\hat{\varepsilon} - 1}{2 \hat{\varepsilon} \lambda} C_u \kappa \left[\left(\hat{\varepsilon} + \frac{C_u}{C_d} \right) \frac{\gamma}{C_u \kappa} - \frac{\dot{T}_a}{\dot{T}_s} \right] \right\} \lambda \\
659 \quad &= \left\{ \frac{C_u}{\lambda} \frac{\dot{F}'}{\dot{T}_s} + \frac{\hat{\varepsilon} + 1}{2 \hat{\varepsilon}} - \frac{\hat{\varepsilon} - 1}{2 \hat{\varepsilon}} \frac{C_u \kappa}{\lambda} \left[\left(\hat{\varepsilon} + \frac{C_u}{C_d} \right) \frac{\gamma}{C_u \kappa} - \frac{\dot{T}_a}{\dot{T}_s} \right] \right\} \lambda \\
660 \quad &= \left\{ -\frac{C_u}{|\lambda|} \frac{\dot{F}'}{\dot{T}_s} + \frac{\hat{\varepsilon} + 1}{2 \hat{\varepsilon}} + \frac{\hat{\varepsilon} - 1}{2 \hat{\varepsilon}} \frac{C_u \kappa}{|\lambda|} \left[\left(\hat{\varepsilon} + \frac{C_u}{C_d} \right) \frac{\gamma}{C_u \kappa} - \frac{\dot{T}_a}{\dot{T}_s} \right] \right\} \lambda
\end{aligned}$$

$$663 \quad \frac{\dot{N}}{\dot{T}_u} = \left\{ -\frac{C_u}{|\lambda|} \frac{\dot{F}'}{\dot{T}_s} + \frac{\hat{\varepsilon} + 1}{2 \hat{\varepsilon}} \left(1 + \frac{\hat{\varepsilon} - 1}{\hat{\varepsilon} + 1} \frac{C_u \kappa}{|\lambda|} \left[\left(\hat{\varepsilon} + \frac{C_u}{C_d} \right) \frac{\gamma}{C_u \kappa} - \frac{\dot{T}_a}{\dot{T}_s} \right] \right) \right\} \lambda \quad (\text{A15})$$

665 The term in square brackets in equation (A15) is the key term that provides a NT -diagram with
666 evolving slope when the forcing is constant. The second part of this term provides the temporal

667 evolution, whereas the first part is a constant term that sets the base enhancement of the slope.
 668 Interestingly, this first part contains in particular the thermal capacities of the system.

669 If I rewrite this first part of the square-brackets term, the terms are shown clearly

$$670 \quad \frac{\dot{N}}{\dot{T}_u} = \left\{ -\frac{C_u \dot{F}'}{|\lambda| \dot{T}_s} + \frac{\hat{\varepsilon} + 1}{2\hat{\varepsilon}} + \frac{\hat{\varepsilon} - 1}{2\hat{\varepsilon}} \frac{C_u \kappa}{|\lambda|} \left[\left(\frac{\hat{\varepsilon}}{C_u} + \frac{1}{C_d} \right) \frac{\gamma}{\kappa} - \frac{\dot{T}_a}{\dot{T}_s} \right] \right\} \lambda \quad (A16)$$

671

672 Now in the first part it is the sum of the inverse of the thermal capacities as if we have an electrical
 673 circuit with capacitors in series. Having such a term in the equation for the slope favors the physical
 674 interpretation in terms of thermal capacities, instead of variable feedback mechanisms. The time-
 675 evolving ratio term in the second part, that represents the dynamics of the atmosphere-ocean
 676 coupling, only strengthens this interpretation.

677 As a corollary, if the forcing is constant and $\hat{\varepsilon} \rightarrow 1$, then we recover the classical linear
 678 dependence of the imbalance on T_u

$$679 \quad \lim_{\hat{\varepsilon} \rightarrow 1} \frac{\dot{N}}{\dot{T}_u} = \lambda, \quad F = \text{const}$$

680

681 **Symmetric and antisymmetric modes**

682 From equations (A13), we see that the symmetric and antisymmetric modes are the basis for
 683 the description of the solutions. Thus, let us give some explicit expression for the symmetric and
 684 antisymmetric modes.

707 $\cosh x \pm \sinh x$. The factors within square brackets in the last two terms can be thought as
708 $e^x I_+ \pm e^{-x} I_-$, where I_{\pm} are the corresponding integrals. Using the expression of the exponential
709 function in terms of the hyperbolic functions, I expand $e^x I_+ \pm e^{-x} I_- = (\cosh x + \sinh x) I_+ \pm (\cosh x -$
710 $\sinh x) I_- = (I_+ \pm I_-) \cosh x + (I_+ \mp I_-) \sinh x$. Then, I overcome the limitation and now the two
711 terms are written with hyperbolic functions. The coefficients of the hyperbolic functions are simple
712 combinations of the integrals which can be also expanded easily. I do that now

$$\begin{aligned}
713 \quad I_+ + I_- &= \int_{t_0}^t F' e^{-\mu_+(\tau-t_0)} d\tau + \int_{t_0}^t F' e^{-\mu_-(\tau-t_0)} d\tau = \int_{t_0}^t F' [e^{-\mu_+(\tau-t_0)} + e^{-\mu_-(\tau-t_0)}] d\tau \\
714 &= \int_{t_0}^t F' e^{-(\hat{\lambda}/2)(\tau-t_0)} [e^{-(\kappa/2)(\tau-t_0)} + e^{(\kappa/2)(\tau-t_0)}] d\tau \\
715 &= 2 \int_{t_0}^t F' e^{-(\hat{\lambda}/2)(\tau-t_0)} \cosh \left[\frac{\kappa}{2} (\tau - t_0) \right] d\tau \\
716 \quad I_+ - I_- &= \int_{t_0}^t F' e^{-\mu_+(\tau-t_0)} d\tau - \int_{t_0}^t F' e^{-\mu_-(\tau-t_0)} d\tau = \int_{t_0}^t F' [e^{-\mu_+(\tau-t_0)} - e^{-\mu_-(\tau-t_0)}] d\tau \\
717 &= \int_{t_0}^t F' e^{-(\hat{\lambda}/2)(\tau-t_0)} [e^{-(\kappa/2)(\tau-t_0)} - e^{(\kappa/2)(\tau-t_0)}] d\tau \\
718 &= -2 \int_{t_0}^t F' e^{-(\hat{\lambda}/2)(\tau-t_0)} \sinh \left[\frac{\kappa}{2} (\tau - t_0) \right] d\tau \\
719
\end{aligned}$$

720 If one collects terms corresponding to each hyperbolic function in the former expressions for the
721 normal modes, obtains the following

$$722 \quad T_s = \frac{e^{(\hat{\lambda}/2)(t-t_0)}}{\kappa} \left\{ C_1 \cosh \left[\frac{\kappa}{2} (t - t_0) \right] + C_2 \sinh \left[\frac{\kappa}{2} (t - t_0) \right] \right\} \quad (\text{A17})$$

$$723 \quad T_a = \frac{e^{(\hat{\lambda}/2)(t-t_0)}}{\kappa} \left\{ C_2 \cosh \left[\frac{\kappa}{2} (t - t_0) \right] + C_1 \sinh \left[\frac{\kappa}{2} (t - t_0) \right] \right\} \quad (\text{A18})$$

725 where

$$\begin{aligned}
726 \quad C_1 &= \kappa T_{u,0} \\
727 &\quad - (\hat{\lambda} + 2\gamma'_d) \int_{t_0}^t F' e^{-(\hat{\lambda}/2)(\tau-t_0)} \sinh \left[\frac{\kappa}{2} (\tau - t_0) \right] d\tau + \kappa \int_{t_0}^t F' e^{-(\hat{\lambda}/2)(\tau-t_0)} \cosh \left[\frac{\kappa}{2} (\tau - t_0) \right] d\tau \\
728 \quad C_2 &= (\hat{\lambda} + 2\gamma'_d) T_{u,0} + 2\hat{\epsilon}\gamma'_d T_{d,0} \\
729 &\quad + (\hat{\lambda} + 2\gamma'_d) \int_{t_0}^t F' e^{-(\hat{\lambda}/2)(\tau-t_0)} \cosh \left[\frac{\kappa}{2} (\tau - t_0) \right] d\tau - \kappa \int_{t_0}^t F' e^{-(\hat{\lambda}/2)(\tau-t_0)} \sinh \left[\frac{\kappa}{2} (\tau - t_0) \right] d\tau \\
730
\end{aligned}$$

731 These expressions for the normal modes are quite elegant, and the coefficients C_i summarize
 732 all the information from the initial conditions and the forcing. The initial condition terms in the
 733 C_i correspond to the non-forced response of the system, while the part that is forcing-dependent
 734 corresponds to the forced response of the system.

735 **Forced response to constant forcing**

736 If $F' = F'_c \neq 0$ for $t > t_0$ with F'_c constant and $T_{u,0}, T_{d,0} = 0$ for $t = t_0$, then

$$737 \quad C_1 = F'_c \left\{ -(\hat{\lambda} + 2\gamma'_d) \int_{t_0}^t e^{-(\hat{\lambda}/2)(\tau-t_0)} \sinh \left[\frac{\kappa}{2}(\tau - t_0) \right] d\tau + \kappa \int_{t_0}^t e^{-(\hat{\lambda}/2)(\tau-t_0)} \cosh \left[\frac{\kappa}{2}(\tau - t_0) \right] d\tau \right\}$$

$$738 \quad C_2 = F'_c \left\{ (\hat{\lambda} + 2\gamma'_d) \int_{t_0}^t e^{-(\hat{\lambda}/2)(\tau-t_0)} \cosh \left[\frac{\kappa}{2}(\tau - t_0) \right] d\tau - \kappa \int_{t_0}^t e^{-(\hat{\lambda}/2)(\tau-t_0)} \sinh \left[\frac{\kappa}{2}(\tau - t_0) \right] d\tau \right\} \blacksquare$$

740 where the integrals are easily computed

$$741 \quad \int_{t_0}^t e^{-(\hat{\lambda}/2)(\tau-t_0)} \sinh \left[\frac{\kappa}{2}(\tau - t_0) \right] d\tau = \frac{e^{-(\hat{\lambda}/2)(t-t_0)}}{\lambda'\gamma'_d} \left\{ \frac{\kappa}{2} \cosh \left[\frac{\kappa}{2}(t - t_0) \right] + \frac{\hat{\lambda}}{2} \sinh \left[\frac{\kappa}{2}(t - t_0) \right] \right\} - \frac{\kappa}{2\lambda'\gamma'_d}$$

$$742 \quad \int_{t_0}^t e^{-(\hat{\lambda}/2)(\tau-t_0)} \cosh \left[\frac{\kappa}{2}(\tau - t_0) \right] d\tau = \frac{e^{-(\hat{\lambda}/2)(t-t_0)}}{\lambda'\gamma'_d} \left\{ \frac{\hat{\lambda}}{2} \cosh \left[\frac{\kappa}{2}(t - t_0) \right] + \frac{\kappa}{2} \sinh \left[\frac{\kappa}{2}(t - t_0) \right] \right\} - \frac{\hat{\lambda}}{2\lambda'\gamma'_d} \blacksquare$$

744 and, upon reduction, the C_i are

$$745 \quad C_1 = \frac{F'_c}{\lambda'} e^{-(\hat{\lambda}/2)(t-t_0)} \left\{ -\kappa \cosh \left[\frac{\kappa}{2}(t - t_0) \right] + (2\lambda' - \hat{\lambda}) \sinh \left[\frac{\kappa}{2}(t - t_0) \right] + \kappa e^{(\hat{\lambda}/2)(t-t_0)} \right\}$$

$$746 \quad C_2 = \frac{F'_c}{\lambda'} e^{-(\hat{\lambda}/2)(t-t_0)} \left\{ -(2\lambda' - \hat{\lambda}) \cosh \left[\frac{\kappa}{2}(t - t_0) \right] + \kappa \sinh \left[\frac{\kappa}{2}(t - t_0) \right] + (2\lambda' - \hat{\lambda}) e^{(\hat{\lambda}/2)(t-t_0)} \right\}$$

748 with these expressions is easy to evaluate the terms inside the curly brackets in equations (A17)
 749 and (A18) and the symmetric and antisymmetric modes are (for $t \geq t_0$)

$$750 \quad T_s = \frac{F_c}{\lambda} \left\{ e^{(\hat{\lambda}/2)(t-t_0)} \left(\cosh \left[\frac{\kappa}{2}(t - t_0) \right] + \frac{2\lambda' - \hat{\lambda}}{\kappa} \sinh \left[\frac{\kappa}{2}(t - t_0) \right] \right) - 1 \right\} \quad (\text{A19})$$

$$751 \quad T_a = \frac{F_c}{\lambda} \left\{ e^{(\hat{\lambda}/2)(t-t_0)} \left(\frac{2\lambda' - \hat{\lambda}}{\kappa} \cosh \left[\frac{\kappa}{2}(t - t_0) \right] + \sinh \left[\frac{\kappa}{2}(t - t_0) \right] \right) - \frac{2\lambda' - \hat{\lambda}}{\kappa} \right\} \quad (\text{A20})$$

753 where $F'_c := F_c/C_u$. I can also obtain the explicit time derivatives of both modes. We take the time
 754 derivative both equations (A19) and (A20)

$$\begin{aligned}
 755 \quad \dot{T}_s &= \frac{F_c}{\lambda} e^{(\hat{\lambda}/2)(t-t_0)} \left\{ \frac{\hat{\lambda}}{2} \left(\cosh \left[\frac{\kappa}{2}(t-t_0) \right] + \frac{2\lambda' - \hat{\lambda}}{\kappa} \sinh \left[\frac{\kappa}{2}(t-t_0) \right] \right) \right. \\
 756 &\quad \left. + \frac{\kappa}{2} \left(\frac{2\lambda' - \hat{\lambda}}{\kappa} \cosh \left[\frac{\kappa}{2}(t-t_0) \right] + \sinh \left[\frac{\kappa}{2}(t-t_0) \right] \right) \right\} \\
 757 &= \frac{F_c}{\lambda} e^{(\hat{\lambda}/2)(t-t_0)} \left\{ \lambda' \cosh \left[\frac{\kappa}{2}(t-t_0) \right] + \frac{\lambda' \hat{\lambda} + 2\gamma'_d \lambda'}{\kappa} \sinh \left[\frac{\kappa}{2}(t-t_0) \right] \right\} \\
 758 &= \frac{F_c}{C_u} e^{(\hat{\lambda}/2)(t-t_0)} \left\{ \cosh \left[\frac{\kappa}{2}(t-t_0) \right] + \frac{\hat{\lambda} + 2\gamma'_d}{\kappa} \sinh \left[\frac{\kappa}{2}(t-t_0) \right] \right\} \\
 759 \quad \dot{T}_a &= \frac{F_c}{\lambda} e^{(\hat{\lambda}/2)(t-t_0)} \left\{ \frac{\hat{\lambda}}{2} \left(\frac{2\lambda' - \hat{\lambda}}{\kappa} \cosh \left[\frac{\kappa}{2}(t-t_0) \right] + \sinh \left[\frac{\kappa}{2}(t-t_0) \right] \right) \right. \\
 760 &\quad \left. + \frac{\kappa}{2} \left(\cosh \left[\frac{\kappa}{2}(t-t_0) \right] + \frac{2\lambda' - \hat{\lambda}}{\kappa} \sinh \left[\frac{\kappa}{2}(t-t_0) \right] \right) \right\} \\
 761 &= \frac{F_c}{\lambda} e^{(\hat{\lambda}/2)(t-t_0)} \left\{ \frac{\lambda' \hat{\lambda} + 2\gamma'_d \lambda'}{\kappa} \cosh \left[\frac{\kappa}{2}(t-t_0) \right] + \lambda' \sinh \left[\frac{\kappa}{2}(t-t_0) \right] \right\} \\
 762 &= \frac{F_c}{C_u} e^{(\hat{\lambda}/2)(t-t_0)} \left\{ \frac{\hat{\lambda} + 2\gamma'_d}{\kappa} \cosh \left[\frac{\kappa}{2}(t-t_0) \right] + \sinh \left[\frac{\kappa}{2}(t-t_0) \right] \right\} \\
 763 &
 \end{aligned}$$

764 I present both results jointly to show the simplicity of the derivatives

$$\begin{aligned}
 765 \quad \dot{T}_s &= \frac{F_c}{C_u} e^{(\hat{\lambda}/2)(t-t_0)} \left\{ \cosh \left[\frac{\kappa}{2}(t-t_0) \right] + \frac{\hat{\lambda} + 2\gamma'_d}{\kappa} \sinh \left[\frac{\kappa}{2}(t-t_0) \right] \right\} \\
 766 \quad \dot{T}_a &= \frac{F_c}{C_u} e^{(\hat{\lambda}/2)(t-t_0)} \left\{ \frac{\hat{\lambda} + 2\gamma'_d}{\kappa} \cosh \left[\frac{\kappa}{2}(t-t_0) \right] + \sinh \left[\frac{\kappa}{2}(t-t_0) \right] \right\} \\
 767 &
 \end{aligned}$$

768 With these derivatives, I can calculate the ratio of the antisymmetric mode derivative to the
 769 symmetric one that appears in equation (A15)

$$\begin{aligned}
 770 \quad \frac{\dot{T}_a}{\dot{T}_s} &= \frac{\frac{\hat{\lambda} + 2\gamma'_d}{\kappa} \cosh \left[\frac{\kappa}{2}(t-t_0) \right] + \sinh \left[\frac{\kappa}{2}(t-t_0) \right]}{\cosh \left[\frac{\kappa}{2}(t-t_0) \right] + \frac{\hat{\lambda} + 2\gamma'_d}{\kappa} \sinh \left[\frac{\kappa}{2}(t-t_0) \right]} \\
 771 &= \frac{\frac{\hat{\lambda} + 2\gamma'_d}{\kappa} + \tanh \left[\frac{\kappa}{2}(t-t_0) \right]}{1 + \frac{\hat{\lambda} + 2\gamma'_d}{\kappa} \tanh \left[\frac{\kappa}{2}(t-t_0) \right]} \\
 772 &
 \end{aligned}$$

773 Formally, above result have the alternative form

$$774 \quad \frac{\dot{T}_a}{\dot{T}_s} = \tanh \left[\frac{\kappa}{2}(t - t_0) + \operatorname{arctanh} \left(\frac{\hat{\lambda} + 2\gamma'_d}{\kappa} \right) \right]$$

775

776 This is possible only if $|(\hat{\lambda} + 2\gamma'_d)/\kappa| \leq 1$. Let us prove that in our case this follows

$$777 \quad \left| \frac{\hat{\lambda} + 2\gamma'_d}{\kappa} \right| \leq 1$$

$$778 \quad \frac{\hat{\lambda}^2 + 4\gamma'_d\hat{\lambda} + 4\gamma'^2_d}{\hat{\lambda}^2 + 4\gamma'_d\lambda'} \leq 1$$

$$779 \quad \hat{\lambda}^2 + 4\gamma'_d\hat{\lambda} + 4\gamma'^2_d \leq \hat{\lambda}^2 + 4\gamma'_d\lambda'$$

$$780 \quad \hat{\lambda} + \gamma'_d \leq \lambda'$$

$$781 \quad -\hat{\varepsilon}\gamma' \leq 0$$

782

783 the last inequality is always true, since $\hat{\varepsilon}, \gamma'$ are positive constants. Thus,

$$784 \quad \frac{\dot{T}_a}{\dot{T}_s} = \tanh \left[\frac{\kappa}{2}(t - t_0) + \operatorname{arctanh} \left(\frac{\hat{\lambda} + 2\gamma'_d}{\kappa} \right) \right] \quad (\text{A21})$$

785

786 Equation (A21) is an hyperbolic tangent that grows from -1 to 1 in a sigmoidal fashion. It has a
 787 scaling factor that determines how fast it goes from -1 to 1. It also has a shift that sets where the
 788 hyperbolic tangent will cross zero. Both the scaling and shift depend on the thermal and radiative
 789 parameters of the system. Since the shift is negative, after the initial forcing the deep ocean (that
 790 depends on the antisymmetric mode) warms up slower than the upper ocean. At a latter time, the
 791 ratio becomes positive and the contrary happens. The time at which the sign reverses is

$$792 \quad t_1 = t_0 + \frac{2}{\kappa} \operatorname{arctanh} \left| \frac{\hat{\lambda} + 2\gamma'_d}{\kappa} \right|$$

793

794 **Variation of the climate feedback parameter**

795 With the solution shown before, the NT -diagram has a slope

796
$$\frac{\dot{N}}{\dot{T}_u} = \frac{\hat{\varepsilon} + 1}{2\hat{\varepsilon}} \left(1 + \frac{\hat{\varepsilon} - 1}{\hat{\varepsilon} + 1} \frac{C_u \kappa}{|\lambda|} \left[\left(\hat{\varepsilon} + \frac{C_u}{C_d} \right) \frac{\gamma}{C_u \kappa} - \tanh \left(\frac{\kappa}{2} (t - t_0) + \operatorname{arctanh} \left(\frac{\hat{\lambda} + 2\gamma'_d}{\kappa} \right) \right) \right] \right) \lambda \quad (\text{A22})$$

797

798 The factor is composed of terms that are positive except for the ratio term coming from equation
 799 (A21). The negative ratio for $t \in [t_0, t_1)$ clearly generates a more negative slope, whereas for
 800 $t \in (t_1, \infty)$ makes it less negative. At the start one can get the slope

801
$$\frac{\dot{N}}{\dot{T}_u} = \left(1 + (\hat{\varepsilon} - 1) \frac{\gamma}{|\lambda|} \right) \lambda, \quad t = t_0$$

802

803 and at the time of sign reversal

804
$$\frac{\dot{N}}{\dot{T}_u} = \frac{\hat{\varepsilon} + 1}{2\hat{\varepsilon}} \left(1 + \frac{\hat{\varepsilon} - 1}{\hat{\varepsilon} + 1} \left(\hat{\varepsilon} + \frac{C_u}{C_d} \right) \frac{\gamma}{|\lambda|} \right) \lambda, \quad t = t_1$$

805

806 After the sign reversal the factor of λ will only decrease up to

807
$$\lim_{t \rightarrow \infty} \frac{\dot{N}}{\dot{T}_u} = \frac{\hat{\varepsilon} + 1}{2\hat{\varepsilon}} \left(1 + \frac{\hat{\varepsilon} - 1}{\hat{\varepsilon} + 1} \frac{C_u \kappa}{|\lambda|} \left[\left(\hat{\varepsilon} + \frac{C_u}{C_d} \right) \frac{\gamma}{C_u \kappa} - 1 \right] \right) \lambda$$

808

809 Equation (A22) shows the importance of the ratio of the symmetric and antisymmetric modes. Its
 810 physical meaning, the relationship between the upper- and deep-ocean warming, sets the strength
 811 of the variation of the climate feedback, whereas the constant term sets a base enhancement around
 812 which the feedback evolves. The thermal capacities of the system determine this constant term.

813 **APPENDIX B**

814 **Feedbacks and pattern effect in a non-linear planetary budget**

815 I start with a planetary imbalance considering a variation of the planetary thermal capacity

816
$$N = (1 - \alpha)S + G - \epsilon \sigma (fT_u)^4 - \dot{C}T_u \quad (\text{B1})$$

817

818 where S is the incoming solar short-wave flux at the TOA, α is the planetary albedo, G are the
819 remaining natural and anthropogenic energy fluxes, and the last two terms are the planetary long-
820 wave response and the contribution to the radiative response of a varying thermal capacity. As said
821 in the main text, the ocean circulation and the atmosphere-ocean coupling provide the dynamical
822 component of the thermal capacity.

823 If I compute the total derivative of N then

$$824 \quad \dot{N} = [(1 - \alpha)\dot{S} + \dot{G}] - S\dot{\alpha} - \sigma(fT_u)^4\dot{\epsilon} - 4\epsilon\sigma(fT_u)^3(\dot{f}T_u + f\dot{T}_u) - \dot{C}\dot{T}_u - T_u\ddot{C}$$

$$825 \quad = [(1 - \alpha)\dot{S} + \dot{G}] - \mathcal{R}$$

827 Here we can see the first term is the change from a time-evolving forcing. The rest of the terms,
828 \mathcal{R} , are atmospheric feedbacks or the effects of ocean circulation and ocean-atmosphere interaction.
829 The fourth term contains the Planck feedback. Let us compare all the terms of \mathcal{R} in comparison to
830 the Planck feedback term $4\epsilon f\sigma(fT_u)^3\dot{T}_u$

$$831 \quad \mathcal{R} = S\dot{\alpha} + \sigma(fT_u)^4\dot{\epsilon} + 4\epsilon\sigma(fT_u)^3(\dot{f}T_u + f\dot{T}_u) + \dot{C}\dot{T}_u + T_u\ddot{C}$$

$$832 \quad = 4\epsilon f\sigma(fT_u)^3\dot{T}_u \left[\frac{S}{4\epsilon f\sigma(fT_u)^3} \frac{\dot{\alpha}}{\dot{T}_u} + \frac{T_u}{4\epsilon} \frac{\dot{\epsilon}}{\dot{T}_u} + \frac{T_u}{f} \frac{\dot{f}}{\dot{T}_u} + 1 + \frac{\dot{C}}{4\epsilon f\sigma(fT_u)^3} + \frac{T_u}{4\epsilon f\sigma(fT_u)^3} \frac{\ddot{C}}{\dot{T}_u} \right]$$

834 By inserting former expression of \mathcal{R} in the total derivative of the planetary imbalance, reordering
835 and dividing by \dot{T}_u , we get the analogous expression for the slope of the NT -diagrams

$$836 \quad \frac{\dot{N}}{\dot{T}_u} = \left[(1 - \alpha) \frac{\dot{S}}{\dot{T}_u} + \frac{\dot{G}}{\dot{T}_u} \right]$$

$$837 \quad - \left[1 + \frac{S}{4\epsilon f\sigma(fT_u)^3} \frac{\dot{\alpha}}{\dot{T}_u} + \frac{T_u}{4\epsilon} \frac{\dot{\epsilon}}{\dot{T}_u} + \frac{T_u}{f} \frac{\dot{f}}{\dot{T}_u} + \frac{\dot{C}}{4\epsilon f\sigma(fT_u)^3} + \frac{T_u}{4\epsilon f\sigma(fT_u)^3} \frac{\ddot{C}}{\dot{T}_u} \right] 4\epsilon f\sigma(fT_u)^3$$

839 The first contribution in the \mathcal{R}/\dot{T}_u term is 1, representing the Planck feedback. The second
840 contribution is the planetary albedo feedback. It includes the surface albedo feedback as well as
841 the short-wave cloud feedback. The third contribution is the emissivity feedback, to which mainly
842 contributes the traditional water-vapor feedback. The fourth contribution is a representation of the
843 lapse-rate feedback. The fifth and sixth contributions are not atmospheric feedbacks but the effect

844 of the evolving planetary thermal capacity provided by the atmosphere-ocean interaction and the
845 ocean circulation.

846 Both the fifth and sixth contributions measure the effect of a changing planetary thermal capacity.
847 The fifth term should be positive but reduces its contribution towards the equilibrium in view of
848 the modified two-layer model results. In the same context, the sixth contribution should change
849 sign, in analogy to the linearized model results.

850 **References**

851 Arrhenius, S., 1896: On the Influence of Carbonic Acid in the Air upon the Temperature of the
852 Ground. *Philosophical Magazine and Journal of Science*, **41**, 237–276.

853 Budyko, M., 1969: The effect of solar radiation variations on the climate of the Earth. *Tellus*,
854 **21 (5)**, 611–619, <https://doi.org/10.1111/j.2153-3490.1969.tb00466.x>.

855 Callendar, G. S., 1938: The artificial production of carbon dioxide and its influence on temperature.
856 *Quarterly Journal of the Royal Meteorological Society*, **64 (275)**, 223–240, <https://doi.org/10.1002/qj.49706427503>.
857

858 Ceppi, P., and J. M. Gregory, 2017: Relationship of tropospheric stability to climate sensitivity
859 and Earth’s observed radiation budget. *Proc. Natl. Acad. Sci. (USA)*, **114 (50)**, 13 126–13 131,
860 <https://doi.org/10.1073/pnas.1714308114>.

861 Fourier, J.-B. J., 1827: Mémoire sur les Températures du Globe Terrestre et des Espaces Planétaires.
862 *Mémoires d l’Académie Royale des Sciences de l’Institute de France*, **7**, 570–604.

863 Geoffroy, O., D. Saint-Martin, G. Bellon, A. Voldoire, D. J. L. Olivié, and S. Tytéca, 2013a:
864 Transient Climate Response in a Two-Layer Energy-Balance Model. Part II: Representation of
865 the Efficacy of Deep-Ocean Heat Uptake and Validation for CMIP5 AOGCMs. *J. Climate*, **26 (6)**,
866 1859–1876, <https://doi.org/10.1175/JCLI-D-12-00196.1>.

867 Geoffroy, O., D. Saint-Martin, D. J. L. Olivié, A. Voldoire, G. Bellon, and S. Tytéca, 2013b:
868 Transient Climate Response in a Two-Layer Energy-Balance Model. Part I: Analytical Solution
869 and Parameter Calibration Using CMIP5 AOGCM Experiments. *J. Climate*, **26 (6)**, 1841–1857,
870 <https://doi.org/10.1175/JCLI-D-12-00195.1>.

871 Gregory, J. M., and Coauthors, 2004: A new method for diagnosing radiative forcing and climate
872 sensitivity. *Geophys. Res. Lett.*, **31** (3), L03 205, <https://doi.org/10.1029/2003GL018747>.

873 Hansen, J. E., R. A. Ruedy, M. Sato, and K.-W. K. Lo, 2010: Global surface temperature change.
874 *Reviews of Geophysics*, **48** (4), RG4004, <https://doi.org/10.1029/2010RG000345>, URL <https://doi.org/10.1029/2010RG000345>.
875

876 Hansen, J. E., G. Russell, A. Lacis, I. Fung, D. Rind, and P. Stone, 1985: Climate Response
877 Times: Dependence on Climate Sensitivity and Ocean Mixing. *Science*, **229** (4716), 857–859,
878 <https://doi.org/10.1002/2017MS001208>.

879 Held, I. M., M. Winton, K. Takahashi, T. Delworth, F. Zeng, and G. K. Vallis, 2010: Probing the
880 Fast and Slow Components of Global Warming by Returning Abruptly to Preindustrial Forcing.
881 *J. Climate*, **23** (9), 2418–2427, <https://doi.org/10.1175/2009JCLI3466.1>.

882 Hu, S., S.-P. Xie, , and S. M. Kang, 2021: Global Warming Pattern Formation: The Role of Ocean
883 Heat Uptake. *J. Climate*, **35** (6), 1885–1899, <https://doi.org/10.1175/JCLI-D-21-0317.1>.

884 Jiménez-de-la-Cuesta, D., 2022a: diegojco/pattern-effect: Preprint release. *Software in Github*,
885 <https://doi.org/10.5281/zenodo.6530577>.

886 Jiménez-de-la-Cuesta, D., 2022b: Global and tropical band averages for a selection of CMIP5 and
887 CMIP6 models: piControl and abrupt-4xCO2 experiments. *Dataset in Zenodo*, <https://doi.org/10.5281/zenodo.6531208>.
888

889 Kiehl, J., 2007: Twentieth century climate model response and climate sensitivity. *Geophys. Res.*
890 *Lett.*, **34** (22), L22 710, <https://doi.org/10.1029/2007GL031383>.

891 Mauritsen, T., 2016: Clouds cooled the Earth. *Nat. Geosci.*, **9** (12), 865–867, <https://doi.org/10.1038/ngeo2838>.
892

893 Meraner, K., T. Mauritsen, and A. Voigt, 2013: Robust increase in equilibrium climate
894 sensitivity under global warming. *Geophys. Res. Lett.*, **40** (2), 5944–5948, <https://doi.org/10.1002/2013GL058118>.
895

- 896 Newsom, E., L. Zanna, S. Khatiwala, and J. M. Gregory, 2020: The Influence of Warming Patterns
897 on Passive Ocean Heat Uptake. *Geophys. Res. Lett.*, **47 (18)**, e2020GL088429, [https://doi.org/](https://doi.org/10.1029/2020GL088429)
898 10.1029/2020GL088429.
- 899 Rohrschneider, T., B. Stevens, and T. Mauritsen, 2019: On simple representations of the climate
900 response to external radiative forcing. *Climate Dyn.*, **3 (5-6)**, 3131–3145, [https://doi.org/10.](https://doi.org/10.1007/s00382-019-04686-4)
901 1007/s00382-019-04686-4.
- 902 Rugenstein, M. A. A., and K. C. Armour, 2021: Three Flavors of Radiative Feedbacks and
903 Their Implications for Estimating Equilibrium Climate Sensitivity. *Geophys. Res. Lett.*, **48 (15)**,
904 e2021GL092983, <https://doi.org/10.1029/2021GL092983>.
- 905 Senior, C. A., and J. F. B. Mitchell, 2000: The time-dependence of climate sensitivity. *Geophys.*
906 *Res. Lett.*, **27 (17)**, 2685–2688, <https://doi.org/10.1029/2000GL011373>.
- 907 Talley, L. D., 2015: Closure of the Global Overturning Circulation Through the Indian, Pacific,
908 and Southern Oceans: Schematics and Transports. *Oceanography*, **26 (1)**, 80–97, [https://doi.org/](https://doi.org/10.5670/oceanog.2013.07)
909 10.5670/oceanog.2013.07.
- 910 Winton, M., K. Takahashi, and I. M. Held, 2010: Importance of Ocean Heat Uptake Effi-
911 cacy to Transient Climate Change. *J. Climate*, **23 (9)**, 2333–2344, [https://doi.org/10.1175/](https://doi.org/10.1175/2009JCLI3139.1)
912 2009JCLI3139.1.
- 913 Yuan-Jen, L., Y.-T. Hwang, L. Jian, F. Liu, and B. E. J. Rose, 2021: The Dominant Contribution
914 of Southern Ocean Heat Uptake to Time-Evolving Radiative Feedback in CESM. *Geophys. Res.*
915 *Lett.*, **48 (9)**, e2021GL093302, <https://doi.org/10.1029/2021GL093302>.
- 916 Zhou, C., M. D. Zelinka, and S. A. Klein, 2016: Impact of decadal cloud variations on the Earth's
917 energy budget. *Nat. Geosci.*, **9 (12)**, 871–874, <https://doi.org/10.1038/ngeo2828>.